

Learning from Friends in a Pandemic: Social Networks and the Macroeconomic Response of Consumption

Christos A. Makridis and Tao Wang ^{*}

June 19, 2023

Abstract

Households often learn about the macroeconomy through social communications. We show how communication via social networks allows idiosyncratic shocks to propagate into meaningful macroeconomic responses. We first motivate such a mechanism by showing the responses of daily consumption spending of U.S. counties to plausibly exogenous variations in their social-network exposure to the COVID-19 conditions of geographically remote regions. Various identification strategies confirm that the detected consumption responses were primarily through the channel of expectations, rather than preference interdependence or physical infection risks. Then, we incorporate a belief formation mechanism through social networks into an otherwise standard heterogeneous-agent consumption model. We show that a pandemic-augmented version of this model, where infections initially hit a fraction of more connected regions and gradually propagated via social networks, produces macroeconomic dynamics more aligned with the empirical patterns of aggregate consumption and cross-sectional variations. We also show that such a mechanism is more relevant when the initial shocks hit the more connected agents and when the influences are more dispersed in the network.

Keywords: Aggregate Demand, Consumption, COVID-19, Expectations, Social Networks

JEL Codes: D14, E21, E71, G51

^{*}Christos: Columbia Business School and Stanford University, cmakridi@stanford.edu; Tao: John Hopkins University, twang80@jhu.edu. We would like to thank Safegraph, Facteus and Facebook (especially Mike Bailey) for providing the access to the data used in this paper. We also thank Nick Bloom, Chris Carroll, Laura Veldkamp, Johannes Stroebel, and Jonathan Wright for comments. These views are our own and do not reflect those of any affiliated institutions. GitHub of the project: <https://github.com/iworld1991/FriendsPandemic>.

1 Introduction

Household expectations are increasingly recognized as a central driver of aggregate macroeconomic activity,¹ but much less is known about their determinants, especially how social networks can transmit shocks. In particular, individuals may adjust their consumption as a function of not only direct shocks and changes in their information set, but also what their friends convey to them, particularly with the growing importance of social media (Westerman et al., 2014; Ritter, 2020).

Unfortunately, isolating the role of social networks is challenging because of the “reflection problem” (Manski, 1993, 2000): fluctuations in individual consumption may simply reflect unobserved and correlated shocks to others in their same social network. We overcome these standard challenges by leveraging the COVID-19 pandemic as a shock to pre-existing social ties, building a heterogeneous agents model consistent with the data to conduct counterfactual simulations over the role of social networks in explaining changes in consumption and aggregate activity. Unlike the bulk of contributions thus far that have focused on first-moment shocks,² we explicitly model expectations and social networks to quantitatively evaluate how information travels and influences consumption. While our model is calibrated to data from 2021-2021 to exploit variation from COVID-19, our model could be used to study a wide array of social phenomena. Understanding how information transmits across the social network, influences individual beliefs, and in turn affects aggregate consumption, is especially important in an era of high uncertainty and politicization (Dietrich et al., 2022; Canes-Wrone et al., 2022; Baker et al., 2020a; Eichenbaum et al., 2022).

The first part of our paper provides reduced-form evidence that information propagated through

¹For a relatively small yet actively expanding literature on social mechanisms on economic expectations, see, for example, Shiller and Pound (1989); Hirshleifer et al. (2023) on stock investment, Carroll (2003) on inflation expectations, and Piazzesi and Schneider (2009), Burnside et al. (2016), Bailey et al. (2018a), Bailey et al. (2019) on housing investment and mortgage choices. Carroll and Wang (2023) does an extensive survey of this literature.

²See Krueger et al. (2022), Coibion et al. (2020a), Bartik et al. (2020), Cajner et al. (2020), Baker et al. (2020b), Coibion et al. (2020b), Eichenbaum et al. (2022), Makridis and Hartley (2020) and Guerrieri et al. (2020).

social networks has an effect on consumption. Using a combination of transaction-level data of 5.18 million consumers from Facteus and the Social Connectedness Index (SCI) from Facebook (Bailey et al., 2018a), we find that a 10% increase in SCI-weighted cases and deaths is associated with a 0.15% and 0.42% decline in consumption, respectively. We also find that these declines are greater among social-contact-based consumption categories and activities away from home. For instance, each 10% increase in SCI-weighted cases is associated with a 0.5% decrease in clothing, footwear, and cosmetics, a 1.1% decrease in contract-based service, and a 1.2% decrease in travel. These decreases are two-to-three times as large as the drop in average spending. We implement several robustness exercises. First, we control for state \times day fixed effects, which isolates variation across counties in the same state. Furthermore, we show that increases in SCI-weighted infections are associated with stronger declines in consumption when stay-at-home orders are in place. This is consistent with the idea that online social networks are more influential when consumers are unable to gather information through local in-person communications. Second, we conduct a wide array of heterogeneity exercises, showing that the heterogeneous treatment effects align with theory (e.g., greater effect in younger counties since social networks are more prevalent with millennials). Finally, we exploit counties' heterogeneous exposure to day-to-day changes in infections in South Korea, Italy, France, and Spain. We find similar results even when we restrict our sample to days between February 15th and March 15th 2020 prior to the U.S. national pandemic response.

The second part of the paper constructs a tractable model of social-network-based learning in which agents both learn from respective local news and communicate their posterior beliefs about an aggregate hidden state via a network. The model combines various existing models of expectation formation at the individual level with “naive learning” (DeGroot, 1974; DeMarzo et al., 2003) at the social level.³ Naive learning assumes that individuals’ partial belief updating is a weighted

³For instance, diagnostic expectations (Bordalo et al., 2020), and information rigidity (Coibion and Gorodnichenko, 2015a).

average of their friends' posteriors, and the relative weights are proportional to the strength of the interpersonal ties. Due to asymmetric influences of different agents in the network, naive learning results in additional inefficiency in information aggregation. This also allows idiosyncratic shocks to be gradually propagated into society and has persistent aggregate belief effects. Such effects are especially salient when the shocks hit the most connected locations and when the agents have more dispersed influences. We integrate this social-communication mechanism into a pandemic-augmented quantitative consumption model featuring market incompleteness. We assume that individuals learn about the imperfectly observable aggregate transmission of COVID-19 via changes in local infections and then communicate their beliefs via a network, reflecting the gradual spread of information and beliefs over the course of the pandemic. Meanwhile, local infections also negatively affect income and preferences toward contact-based consumption.

After matching the pre-pandemic cross-sectional consumption inequality and externally estimated dynamics of infection, our model generates economically significant impacts of the social network on the consumption responses. For instance, following a one-time 10% increase in local infections to the top one-third “influencers” in the economy, a medium degree of social communication in the model moderated the initial cut in spending by 0.5 percentage points compared to the scenario of zero social communication. This is economically meaningful: it corresponds to a difference of 5 percentage points in terms of the consumption responses to a standard permanent income shock. Our results also help explain the slow recovery of consumption due to the stickiness in belief adjustment induced by social communications. In addition, a higher dispersion in influence in the social network in 2019, relative to in 2016, also explains the the observed aggregate consumption responses. In sum, our model shows how social networks can propagate the effects of idiosyncratic shocks and generate consumption dynamics that are more consistent with the empirical regularities.

Our paper most closely contributes to an emerging series of studies on the effects of social

networks on economic decisions (Bailey et al., 2018a, 2019, 2022a; Makridis, 2022). Unlike the large body of work on peer-effects via preference dependence, this literature emphasizes the role of influence channeled via expectations/beliefs, although direct evidence using belief data remains rare. Closely related to our paper is Eichenbaum et al. (2022), showing how accounting for consumer expectations about COVID-19 can explain the decline in expenditures. Our empirical results show similar effects as these studies, but we take one step further to build a model of belief formation reflecting social influences and apply it to a macroeconomic setting. We show it has important implications for the macroeconomic response and dynamics following shocks. Although we have calibrated it to a COVID-19 setting, the model is general and provides a handy framework to incorporate social-network-based learning in different macroeconomic settings such as the housing market, where social communication has a large role to play in driving aggregate beliefs in the presence of local and aggregate news (Burnside et al., 2016; Bayer et al., 2021).

Our work is also related to a line of theoretical work on social learning that mostly focuses on equilibrium and asymptotic properties like the naive learning originally formulated by DeGroot (1974), Friedkin and Johnsen (1999) and DeMarzo et al. (2003). Further extensions of these models also explore the existence of the “wisdom of crowds” (Golub and Jackson, 2010) and the spread of misinformation (Acemoglu et al., 2010). Our model modifies their formulation into a dynamic setting, with newly arriving signals used for private updating. More importantly, our focuses are on dynamics and responses to local and aggregate shocks and how it is translated into aggregate belief changes and outcomes instead of long-run properties. We think this is especially relevant for understanding how to quantitatively model macroeconomic shock propagation mechanisms.

In addition, we directly contribute to a large literature on the household response of consumption to macroeconomic shocks, which focuses on the impact of income volatility and borrowing constraints (Zeldes, 1989; Pistaferri, 2001; Gourinchas and Parker, 2002), stimulus (Di Maggio

et al., 2017; Fuster et al., 2018), tax rebates (Souleles, 1999; Johnson et al., 2006; Agarwal et al., 2007), sentiment(Carroll et al., 1994; Gillitzer and Prasad, 2018) on consumption. Quantifying how shocks affect consumption is important for understanding the presence of partial insurance and the pass-through of shocks (Blundell et al., 2008; Kaplan and Violante, 2010, 2014; Heathcote et al., 2014).⁴ Our results highlight how social communication and information transmits these shocks in a more realistic setting of imperfect information and individual over (under)reactions.

Finally, our paper is related to an emerging empirical literature on the role of personal experience in expectation formation. Studies have highlighted the role of personal experience in forming beliefs about future returns (Cogley and Sargent, 2008), inflation (Malmendier and Nagel, 2016; Coibion and Gorodnichenko, 2015b), energy prices (Binder and Makridis, 2020), housing prices (Kuchler and Zafar, 2019), macroeconomic activity (Malmendier and Nagel, 2011; Makridis, 2022; Makridis and McGuire, 2020), asset prices (Malmendier et al., 2018), political preferences (Giuliano and Spilimbergo, 2014), and consumption (Malmendier and Shen, 2021). Our evidence on social communications corroborates this literature as well, as essentially communications are part of the experiences, and it is fair to conjecture that the effects of experiences on expectations are by and large reinforced via interpersonal communications. This is reminiscent of models of macroeconomic expectation formation of average households via interpersonal communications (Carroll, 2003).

2 Data and Measurement

The transaction-level data is provided by Safegraph and Facteus based on an anonymized panel of roughly 5.18 million debit card users' daily spending records between January 1st, 2017 to June 30th, 2020.⁵ Average nationwide daily spending of the whole sample is 194 million dollars from a

⁴See Jappelli and Pistaferri (2010) for a survey.

⁵Transactions are collected from primarily four types of cards providers across the United States: (1) bank debit cards whose majority users are young people, (2) general-purpose debit cards that are primarily distributed by

total of 2.3 million transactions. Despite some limitations, three features make the data particularly useful to our analysis.⁶ First, there is rich geographic heterogeneity. In particular, transactions are partitioned by the residential zipcode of the card user. We then aggregate zip-level transactions into county-level consumption observations of 3051 counties (out of 3141 in the United States as of 2019). For zip zones that are associated with multiple counties, we allocate total consumption to its multiple corresponding counties based on its population weights. To ensure the county-level consumption is not biased by abnormal individual users' records and extreme values, we restrict our sample to include only county-day observations with more than 30 card users. Daily average consumption expenditures per card user is roughly \$40 based on 0.5 transactions.

Second, there is high-frequency variation. In particular, we exploit the daily variation in transactions to identify the response of consumption to news about the pandemic. Since the epidemic crisis has eclipsed nearly ever other national and international event with release of daily news on the number of infections and deaths, daily records provide much cleaner variation than the common alternative of monthly data to recover the effects of news and social media. Although the transaction data goes back to 2017, we restrict the sample to the period between February 1st and June 30th with a total of 152 days and roughly 450,000 county \times day observations. This period spans from the early spreading stage of the COVID-19 in Asian and European continents to the peak of the crisis within the United States. Depending on if the focus of analysis is domestic or international, we split our sample with the cutoff date of March 15—a widely acknowledged watershed in nationwide response to the crisis in the country.

Finally, the spending transaction is recorded by the merchant's type identified by its merchant
merchants and retailers, (3) payroll cards used between employers and employees, and (4) government cards.

⁶One limitation of our data is that the location of a transaction differs from the location of residence; we only observe the latter. While we suspect that exploiting county-level (rather than zipcode-level) variation mitigates this concern, since people consume locally most of the time, we view potential misclassification as a source of measurement error (Chen et al., 2011). This would bias us against finding a result. We nonetheless conduct robustness where we investigate potential heterogeneous treatment effects in areas that have high versus lower levels mobility in "normal times", i.e. college towns.

classification code (MCC), a commonly adopted classification scheme by major card providers such as Visa/Mastercard. This allows us to study the consumption responses by category. We group each one of the 982 MCCs into 16 broad categories based on their degree of exposure to the infection risks.⁷ For instance, eating/drinking/leisure outside the home, contact-based services such as barbershops, and travel are expected to be most severely hit by the infection risk. Grocery and food shopping, financial services, and housing utilities, in contrast, are expected to have mild responses to the pandemic news during this period. In Appendix A.1, we validate that both the category coverage and time-series pattern from our constructed series of consumption represents the pattern in the commonly used macro consumption data series well.

We also draw on the Social Connectedness Index (SCI) from Facebook⁸, introduced originally by Bailey et al. (2018b) to study how information about housing prices is diffused among social networks and affects the decision to rent versus own a home. This data are now used more widely to understand how social ties are related with economic activity (Bailey et al., 2018b) and expectations about macroeconomic activity (Makridis, 2022). The index is constructed from anonymized information between all Facebook users, counting the number of friendship ties between county c and every other county c' in the United States. We use the 2019 data extract. Each user is limited to a total of 5,000 friends on a profile. Network ties require that both sides agree. Finally, we obtain the number of COVID-19 infections and deaths at the county \times day level from the Center for Systems Science and Engineering from Johns Hopkins.⁹

3 Reduced-form Evidence

⁷See Section A.2 in the Online Appendix for examples of merchant types that fall into each category.

⁸Till 2011, there were about 149 million users of Facebook in the U.S. out of the 260-million eligible population, 15.9 billion edges, an average of 214 friend ties per user (Ugander et al. (2011)).

⁹See Figures A.3 and A.4 in Section A.3 of the Online Appendix.

3.1 Identification Strategy

In order to identify an individual county’s consumption responses to heterogeneous information exposure to COVID news, we draw on the Social Connectedness Index (SCI) to produce an SCI-weighted index of COVID-19 cases and deaths:

$$COVID_{c,t}^{SCI} = \sum_{c' \neq c} (COVID_{c',t} \times SCI_{c,c'}) \quad (1)$$

where $COVID_{ct}^{SCI}$ denotes the logged SCI-weighted number of cases or deaths in connected counties, $COVID_{c',t}$ denotes the logged number of cases or deaths in county c' , and $SCI_{c,c'}$ denotes our measure of the SCI. We underscore two important features about our construction of $SCI_{c,c'}$.

First, we omit the number of friendship ties between county c and itself, thereby exploiting only the variation in its exposure to other locations. This means that Equation 1 will not “double count” local infections. Second, we normalize the number of friendship ties in a county to its total number of friendship ties, thereby exploiting the relative exposure to other locations. This means that differences in the level of friendship ties will not explain differences in consumption; only relative differences across counties.¹⁰ Using this SCI-weighted index of the number of cases and deaths, we consider regressions of the following form that also control for local infections:

$$y_{c,t}^k = \gamma COVID_{c,t}^{SCI} + \phi COVID_{c,t} + \zeta_c + \lambda_t + \epsilon_{c,t} \quad (2)$$

where $y_{c,t}^k$ denotes logged consumption for county c on day t for category- k consumption good, and ϕ and λ denote fixed effects on county and day-of-the-year. We cluster standard errors at the

¹⁰For example, suppose that county A has 100 friendship ties with county B and county C. If county D has 1000 ties with both county B and C, then the level of friendship ties would differ, but the relative amount is the same. Because we do not want to confound differences in the level of social media and/or network exposure with consumption, but rather focus on the connectivity to different locations, we normalize our measure. However, we also obtain qualitatively similar results if we leverage the differences in levels too.

county-level to allow for arbitrary degrees of autocorrelation over time.

Our identifying variation in Equation 2 comes from the fact that the social network in a county is pre-determined with respect to the infections that it and others faces over the pandemic. Consider, for example, two counties that share the same population, industrial and occupational composition, and education and age distributions. To the extent that they are both heterogeneously connected to different external counties, then their local response might differ as some residents hear more pessimistic versus optimistic information. We believe that the variation in heterogeneous exposure to other counties is plausibly exogenous. We also consider additional robustness exercises where we exploit the exposure of different *countries* to the pandemic based on their social connectivity before the quarantines began in the United States in March 2020.

3.2 Main Results

Table 1 documents the results associated with Equation 2. We begin with a standard fixed effects estimator in columns 1 and 6, exploit variation within the same county over time. We find that a 10% rise in SCI-weighted cases and deaths are associated with a 0.51% and 0.62% decline in consumption expenditures, respectively. One concern with these results, however, is that we are failing to control for local infections and deaths. If, for example, counties that are relatively more exposed to counties with higher infections also have higher infections themselves in some time-varying way, then we may obtain downward biased coefficient estimate.

To address these concerns, columns 2 and 7 control for logged county cases and deaths. Consistent with our concerns about the potential for bias, our point estimate on the SCI-weighted infections index declines: a 10% rise in SCI-weighted cases and deaths is associated with a 0.15% and 0.42% decline in consumption expenditures respectively. Moreover, increases in contempor-

neous local cases are also associated with declines in consumption, but with a lower magnitude. Local deaths also decrease consumption by a similar degree, but are statistically significant. We have also experimented with one-week and two-week lags on county cases and deaths because of the incubation period for the virus, but the results are not statistically different: if anything, the gradient on SCI-weighted cases is slightly higher.

Yet another concern is that state policies vary considerably over these months. Even though there was a national quarantine, states introduced policies of varying restrictiveness, including stay-at-home orders (SAHOs). For example, [Ali et al. \(2021\)](#) find that the adoption of SAHOs is associated with a persistent decline in job postings for early care and education. This may also impact consumption by shifting the composition of goods and the overall amount of goods as people stay home. Consistent with this interpretation, columns 3 and 8 show that the adoption of a SAHO is associated with a 5.6-5.8% decline in consumption. Moreover, increases in SCI-weighted cases and deaths continue to have a negative association with consumption.

Next, we exploit variation in SAHOs to provide an additional diagnostic into the potential causal interpretation of our estimates. If social networks have a causal mediating effect on consumption, then our estimates should be concentrated in states and days that have enacted SAHOs since they keep individuals in doors where they are more likely to rely on social networks for information through, for example, Facebook, rather than through in-person interactions. Consistent with our hypothesis, columns 4 and 9 show that a 10% rise in SCI-weighted cases and deaths following the adoption of a SAHO is associated with an additional a 0.24% and 0.26% decline in consumption expenditures, which is roughly twice the magnitude obtained in columns 2 and 7. These coefficients are also more precisely estimated, significant at the 1% level.

Although we have taken measures to control for local infections and focused on areas with low mobility due to SAHOs, it is still possible to question whether individuals' consumption responses

to online exposures are primarily driven by concerns about immediate physical infection risk in their own neighborhoods. This is because people are more likely to be connected online to others who are physically close to them. To address this concern, we conducted additional analyses in Columns 5 and 10 using alternative SCI-weighted measures that only include connected counties outside the state. Remarkably, we found that the coefficients in these columns remain significantly negative. Specifically, a 10% increase in out-of-state SCI-weighted cases and deaths is associated with a decline in consumption spending of 0.16% and 0.59%, respectively.

Furthermore, to account for the fact that physical proximity extends beyond state borders, we included regression results in Section A.4 of the Appendix, that jointly control for SCI-weighted cases and corresponding measures weighted by physical distances. Importantly, the statistical significance of the coefficients for SCI-weighted cases and deaths remains unchanged in these analyses.

Did the spending responses differ across different types of consumption? If the reactions were mostly due to concerns about the infection risk, instead of about the economic conditions of the connected regions, the responses should be the strongest in the types that bear the highest risk of COVID. We did find that this is the case. Figure 1 documents these results by reporting the coefficients associated with major categories of goods, which we created based on merchant category codes (MCC) in the transaction data. Both the direct effect of infections and the indirect effects of social communications are reported. We find that clothing, footwear, and cosmetic products decline the most, followed by contact-based services, durables, travel, and eating or drinking outside the home. For example, a 10% rise in SCI-weighted infections is associated with nearly a 0.5% decline in clothing, footwear, and cosmetic spending, whereas the effects on grocery/food or home leisure spending are nearly zero. These results are consistent with Coibion et al. (2020b) who find a 31 log point drop in consumer spending concentrated in travel and clothing. Similarly, we see the largest association for contact-based consumption: a 10% rise in SCI-weighted infections is associated with

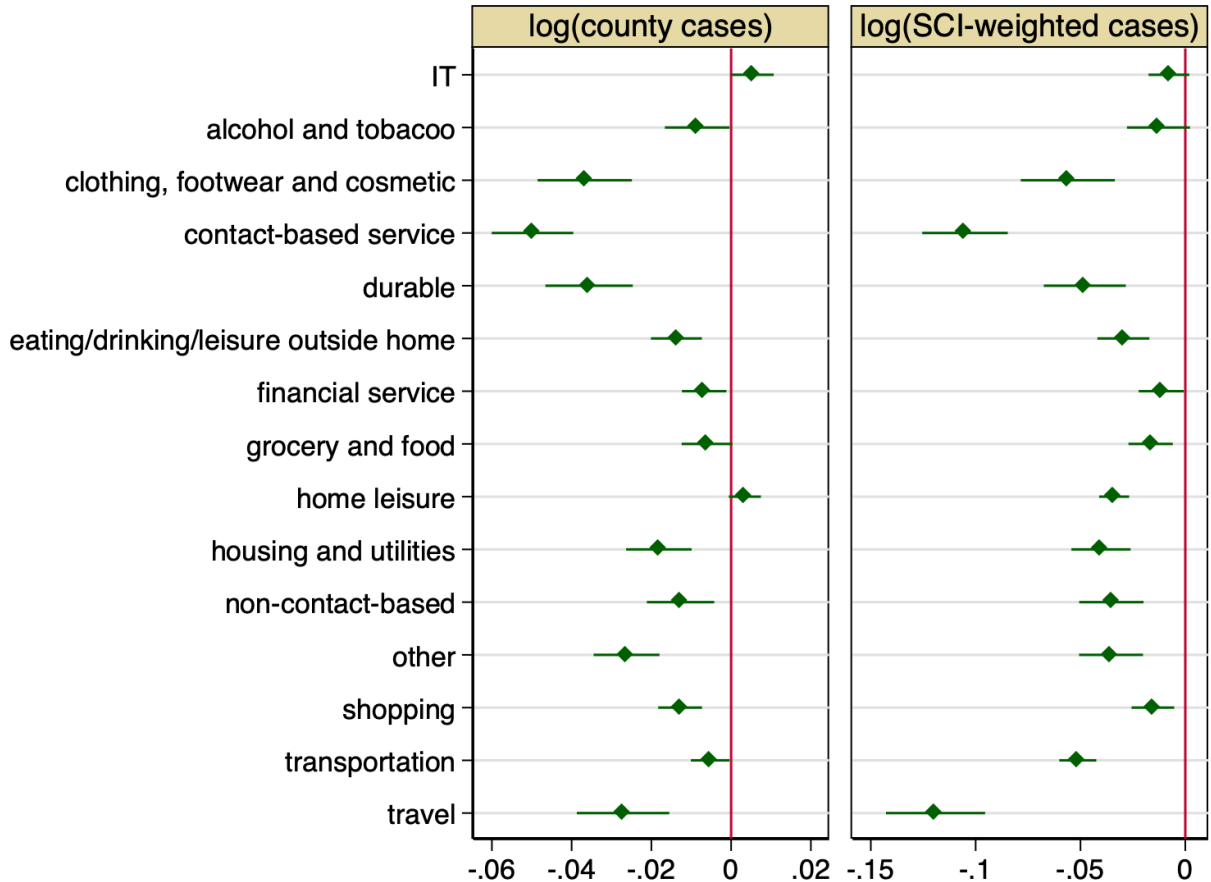
Table 1: Consumption Responses to Increases in Socially-connected Coronavirus Cases and Deaths

Dep. var. =	log(Consumption Expenditures)									
	(1)	(2)	(3)	(4)	(5)	(6)	(7)	(8)	(9)	(10)
Has SAHO			-.058*** [.005]	.007 [.012]	-.058*** [.005]			-.056*** [.005]	-.044*** [.005]	-.060*** [.005]
log(SCI-weighted Cases)	-.051*** [.007]	-.015* [.008]	-.014* [.008]	-.003 [.009]						
× SAHO				-.024*** [.004]						
log(SCI-weighted Deaths)								-.062*** [.008]	-.042*** [.010]	-.063*** [.012]
× SAHO									-.049*** [.013]	-.026*** [.005]
log(SCI-weighted Cases, Other States)							-.016* [.009]			
log(SCI-weighted Deaths, Other States)										-.059*** [.012]
log(County Cases)	-.015*** [.004]	-.006* [.004]	-.006 [.004]		-.006* [.004]			-.013*** [.004]	-.003 [.003]	-.003 [.003]
log(County Deaths)	-.015*** [.004]	-.018*** [.003]	-.018*** [.003]	-.018*** [.003]	-.017*** [.003]			-.006* [.004]	-.008** [.004]	-.007* [.004]
R-squared	.97	.97	.97	.97	.97	.97	.97	.97	.97	.97
Sample Size	351645	351645	351645	351645	351645	351645	351645	351645	351645	351645
County FE	Yes	Yes	Yes	Yes	Yes	Yes	Yes	Yes	Yes	Yes
Time FE	Yes	Yes	Yes	Yes	Yes	Yes	Yes	Yes	Yes	Yes
State Policies	No	No	Yes	Yes	Yes	No	No	Yes	Yes	Yes
State × Month FE	No	No	Yes	Yes	Yes	No	No	Yes	Yes	Yes

Notes – Sources: Facebook Social Connectedness Index (SCI) for 2019, Facteus. The table reports the coefficients associated with regressions of logged consumption spending on logged SCI-weighted infections (excluding county c 's friendship ties with itself) and logged county infections and deaths, conditional on county and time-fixed effects. Consumption is deflated by the national personal consumption expenditure index. Our SCI-weighted cases and death index is constructed as follows: $COVID_{ct}^{SCI} = \sum_{c'} (COVID_{ct}^{SCI} \times SCI_{c,c'})$ where $COVID_{ct}^{SCI}$ denotes the logged SCI-weighted number of cases or deaths in connected counties, $COVID_{ct}^{c,t}$ denotes the logged number of cases or deaths in county c' , and $SCI_{c,c'}$ denotes our measure of the SCI. We normalize the scaled number of friendship ties in a county to its total number of friendship ties, thereby exploiting the relative exposure to other locations. Our variables that are denoted “other states” construct the SCI excluding counties within the same state to control for physical proximity. Standard errors are clustered at the county level. The sample period is between March 1st to June 30th, 2020.

a 1.3% decline in consumption.

Figure 1: Consumption Response to COVID-19 Shocks, by Consumption Category



Notes.—Source: Facebook 2019 Social Connectedness Index (SCI) and Facteus. The figure reports the coefficients associated with regressions of logged consumption in a county on the logged number of COVID-19 cases (Panel A) and the logged number of SCI-weighted cases (Panel B) by category of consumption. Each transaction is classified as one of the following category based on its merchant category code (MCC). The sample period is between March 1st to June 30th, 2020

3.3 Heterogeneous Treatment Effects Across Space

We now turn towards evidence of heterogeneity in the treatment effects by county characteristics.

We control for the direct effects of county infections and deaths, focusing on variation in the SCI-weighted infections. We focus on per capita income, the age distribution, population, the share of digitally-intensive employees as defined by [Gallipoli and Makridis \(2018\)](#), and the share of teleworking employees as defined by [Dingel and Neiman \(2020\)](#). We partition each variable based on the

median value, allowing for heterogeneity above and below the median. Our results with the digital and telework shares are both estimated on a restricted sample because we obtain them from the American Community Survey microdata, which does not cover every county.

Table 2 documents these results. While not all the differences across different types of counties are statistically distinguishable from one another, they are consistent with theory. For example, a 10% rise in the SCI-weighted infections is associated with a 0.47% decline in consumption among the counties below the median in per capita income and a 0.12% decline among the rest. This could be consistent with the presence of greater information asymmetries in lower income counties, so individuals have to rely on more informal networks for information. However, given that our consumption data has better coverage in lower income areas, it is possible that we simply have more measurement error in higher income counties.

Turning towards heterogeneity in the age distribution, we distinguish among those counties that rank above and below the median in terms of the share of individuals below age 35 and the share of individuals above age 65. We do not see statistically different effects when we partition by the median share of individuals below the age of 35: in both cases, a 10% rise in SCI-weighted infections is associated with a 0.21-0.25% decline in consumption. However, when we partition on the median share of individuals over age 65, we find that the elasticity is concentrated in counties with lower shares, implying a 0.28% decline in consumption (compared with a 0.14% decline for counties with higher shares of individuals over the age of 65). This is consistent with the fact that younger individuals are more likely to pay attention to information from social media (Smith and Anderson, 2018). We also find that the effects are concentrated among counties with a larger population.

Finally, we do not see much of a difference between states that rank higher versus lower in terms of digital intensity based on occupational composition (Gallipoli and Makridis, 2018, 2022), but we do see a larger elasticity for states that have a higher share of telework (Dingel and Neiman, 2020).

This could be consistent with the fact that states with more remote workers are likely to rely more on social networks for information, rather than personal experience.

3.4 Understanding the Mechanisms

We have shown that there is an economically and statistically meaningful decline in consumption associated with increases in the number of COVID-19 infections in socially connected counties even after controlling for time invariant characteristics across space and time, as well as time-varying shocks to local health outcomes (e.g., infections and deaths). However, one concern is that these results are plagued by other time-varying omitted variables that jointly affect connected counties and local consumption outcomes. This section provides further evidence that the results reflect a genuine information effect, rather than potential omitted variables.

One of the primary examples of omitted variables bias is the introduction of state-specific policies. For example, one possibility is that the introduction of emergency orders within a state naturally lead to declines in consumption by significantly disrupting foot traffic and leading to closures of businesses. While we show that our results are robust to controlling for state \times day fixed effects, we nonetheless explore this possibility further by exploiting variation in the staggered introduction of state-specific stay-at-home orders (SAHOs) using data from [Ali et al. \(2021\)](#). If, for example, the introduction of SAHOs and other state policies account for the decline in consumption ([Coibion et al., 2020b](#)), then we should see that the effect of the SCI-weighted infections loads on the interaction between it and the SAHOs. However, when we estimate these fixed effect specifications, we find a statistically insignificant point estimate of -0.002. This placebo counters the possibility that there are other unobserved and time-varying county-specific policies that vary with both consumption and connected counties.

Table 2: Heterogeneous Effects of the COVID-19 Information Shock on Consumption, by County Characteristics

RHS Variable Partition =	Per Capita Income		Share Under Age 35		Share Over Age 65		Population		Digital Intensity		Teleworking Intensity	
	High	Low	High	Low	High	Low	High	Low	High	Low	High	Low
log(SCI-weighted Cases)	-.012 [.010]	-.047*** [.014]	-.021** [.010]	-.025** [.011]	-.014 [.012]	-.028*** [.010]	-.044*** [.008]	.007 [.015]	-.040*** [.009]	-.038*** [.012]	-.042** [.009]	-.031*** [.011]
log(County Cases)	-.009 [.006]	-.004 [.005]	-.002 [.005]	-.010 [.007]	-.004 [.007]	-.008 [.005]	-.008 [.005]	-.013*** [.005]	.000 [.007]	-.014* [.007]	-.020*** [.007]	-.013* [.008]
log(County Deaths)	-.021*** [.005]	-.008 [.004]	-.006 [.004]	-.008 [.006]	-.017** [.007]	-.001 [.004]	.008** [.004]	-.039*** [.004]	.019*** [.010]	.011* [.007]	.015** [.007]	.014** [.007]
R-squared	.97	.96	.97	.95	.94	.98	.98	.89	.98	.98	.97	.98
Sample Size	168408	169458	170209	167657	165469	172397	180275	157591	26823	24096	25876	25043
County FE	Yes	Yes	Yes	Yes	Yes	Yes	Yes	Yes	Yes	Yes	Yes	Yes
Time FE	Yes	Yes	Yes	Yes	Yes	Yes	Yes	Yes	Yes	Yes	Yes	Yes

Notes.—Sources: American Community Survey (2014-2018), Facebook Social Connectedness Index (SCI) for 2019, Facteus. The table reports the coefficients associated with regressions of logged consumption spending on logged SCI-weighted infections (excluding county c 's friendship ties with itself) and logged county infections and deaths, conditional on county, time, and state \times month fixed effects, separately for different groups that partition the county (or in the case of digital and telework intensity, the state) based on whether their value ranks above the median of the distribution. Digital and teleworking intensities are obtained from Gallipoli and Makridis (2018) and Dingel and Neiman (2020). Consumption is deflated by the national personal consumption expenditure index. Our SCI-weighted cases and death index is constructed as follows: $COVID_{c,c'}^{SCI} = \sum_{c'} (COVID_{c',t} \times SCI_{c,c'})$ where $COVID_{c,t}^{SCI}$ denotes the logged SCI-weighted number of cases or deaths in connected counties, $COVID_{c',t}$ denotes the logged SCI-weighted number of cases or deaths in county c' , and $SCI_{c,c'}$ denotes our measure of the SCI. We normalize the scaled number of friendship ties in a county to its total number of friendship ties, thereby exploiting the relative exposure to other locations. Standard errors are clustered at the county-level. The sample period is between March 1st to June 30th, 2020.

We further investigate the role of social networks by turning towards measures of international exposure for each county, leveraging the fact that some countries began experiencing the surge in COVID-19 cases much sooner and more severely than the United States. We focus on four countries—South Korea, Italy, Spain, and France—although our results hold on a broader set of countries exposed early on.¹¹ Each of these four countries successively experienced large number of infections in different scale since late February preceding the United States.

We exploit variation along two dimensions. First, counties vary cross-sectionally in their exposure to these countries. For example, whereas Maricopa County in Arizona has an SCI of 142,771 with France, San Francisco has an SCI of 258,825. Second, countries vary in their intensity of COVID-19 shocks. Figure A.5 in the Appendix shows how Italy experienced a sharper and more severe surge in cases than France even though its population is roughly 6 million smaller. We now consider regressions of logged consumption on the product of the cross-sectional exposure to a country and its time series variation in infections, conditional on the usual county and day fixed effects. Importantly, we restrict our sample to the period between February, 15th to March, 15th, which covers the time leading up to the full-scale outbreak in the United States.¹² This allows us to purge variation that is possibly correlated with time-varying shocks in the United States.

Table 3 documents these results. We find that there is a robust negative association between the SCI-weighted number of infections / deaths and consumption for each country. For example, a 10% rise in infections (deaths) in Italy for counties that are more closely connected to Italy is associated with a 0.07% (0.52%) decline in consumption. One reason for the potentially larger coefficient on deaths over infections stems from the way that media covers international deaths more

¹¹Although we would, of course, ideally include China, the Facebook data does not have representative coverage of ties with China because their government prohibits the use of Facebook.

¹²We also conduct the same analysis for the period after March, 15th for a different consideration. Since the Federal government of the U.S. announced the travel ban from Europe in the same week, focusing on this later period potentially shuts down the channel via which socially connected cases posed a real risk of infection. The negative impacts of consumption by SCI weighted cases from each of this country, if any, becomes more significant.

intensively than the number of infections, although we cannot say conclusively. We see broadly similar treatment effects for each country, although they are smaller for France, perhaps because the United States had already witnessed the experience of Asian countries, like South Korea, and Spain and Italy earlier in the month of March.¹³

Our finding that consumption in one county depends on the infections among connected counties—even if they are geographically distant—builds on an emerging literature on social connectedness (Bailey et al., 2018a, 2019, 2022a). However, separately identifying the causal effect of shocks to a network from selection effects is challenging (Goldsmith-Pinkham and Imbens, 2013). Our diagnostics—the combination of domestic and international connectivity—suggest that we are detecting meaningful effects from social networks, rather than just selection effects, but this remains an area of ongoing research. Our paper is also related to recent evidence from Charoenwong et al. (2020) that finds some counties were more likely to adopt social distancing and restrictions measures based on their exposure to Italy and China, although the data on social connectivity to China is confounded by the fact that use of Facebook is blocked within the country.

4 A Model of Learning and Social Networks

4.1 Model Setup

In order to explore if the social influences on individual expectations identified in the previous section have meaningful aggregate implications, we first construct a model of communications via social networks by adapting the “naive learning” framework, as formulated by DeGroot (1974); DeMarzo et al. (2003); Golub and Jackson (2010), to a dynamic macro setting.

¹³Section A.4 of the Online Appendix also presents additional diagnostics that mitigate concerns that our results simply reflect differences in physical distance between connected counties.

Table 3: Consumption Responses to COVID-19 Information from Other Countries

Dep. var. =	log(spending)						
	ITA	ITA	SPA	SPA	FRA	FRA	SK
log(SCI-weighted cases of the country)	-.007*** [.001]		-.008*** [.001]		-.011*** [.001]		-.011*** [.001]
log(SCI-weighted deaths of the country)		-.052*** [.001]		-.072*** [.001]		-.014*** [.001]	-.081*** [.002]
log(County Cases)	-.005 [.003]	.015*** [.004]	-.005 [.003]	.003 [.004]	-.005 [.003]	-.005 [.003]	.012*** [.004]
log(County Deaths)	-.004 [.016]	-.025 [.018]	-.004 [.016]	-.019 [.018]	-.004 [.016]	-.004 [.016]	-.025 [.018]
R-squared	.97	.98	.97	.98	.97	.97	.98
Sample Size	78550	62925	78550	34148	78550	78550	65552
County FE	Yes						
Day FE	No						

Notes.—Sources: Facebook, Facteus. The table reports the coefficients associated with regressions of logged consumption spending on logged SCI-weighted infections or deaths of a given foreign country, conditional on county and time-fixed effects. These SCI-weighted infections/deaths are obtained by taking the time-varying number of infections in country i and multiplying it by the exposure of county c to country i , producing a Bartik-like measure. The four countries are Italy(ITA), Spain (SPA), France (FRA), and South Korea (SK). The sample period is between February 15th and March 15th, 2020. Standard errors are clustered at the county level.

Assume N agents/nodes in the economy (corresponding to counties in our empirically measured social network) are connected through a pre-determined social network. We use the “listening matrix” W with a size of $N \times N$ to represent bilateral influences between any two agents i and j in the network. More specifically, $w_{i,j}$, the i th row and j th column of W , is the share of connections i has with j in total connections of i in the network (corresponding to SCI in our empirical section). It reflects the influence j has on i . If a particular node i has zero social connections with other nodes, then the i th term in the diagonal of W , $w_{i,i} = 1$.

It then follows that each row of W always sum up to 1. The sum of each column of W , denoted as $d_j = \sum_{i=1}^N w_{i,j}$, is what the network literature refers to as the degree of j , and it reflects j ’s overall influence in the network. By construction, the average degree of all nodes is always one, i.e. $\frac{\sum_j^N d_{i,j}}{N} = \frac{\sum_j^N \sum_{i=1}^N w_{i,j}}{N} = 1$. Meanwhile, a higher cross-sectional dispersion in the degrees reflect a higher asymmetry in influence of different nodes in the network. Degree dispersion has been recognized as a key property of the network that matters for aggregate belief dynamics.¹⁴

Agents in the network are learning about an unobservable aggregate state ψ_t (the spreading speed of the virus in our pandemic setting) via both private signals (changes in local infections) and social communications with connected friends. Specifically, assuming a constant weight λ is given to social communication and the rest comes from private updating, the post-communication belief $\tilde{\psi}_{i,t}$ is a weighted sum of privately updated belief $\hat{\psi}_{i,t}$ and socially updated belief $\sum_{j=1}^N w_{i,j} \tilde{\psi}_{j,t-1}$. The latter is the average of posteriors of all connected nodes from $t - 1$ weighted by the degree of influences of each node has on i .¹⁵ λ is one of the key structural parameters in this model. A higher value of λ implies a higher degree of social communications.

¹⁴Figure A.7 in Section A.3 of the Online Appendix plots the empirically observed distribution of degrees based on SCI in 2016 and 2019.

¹⁵This is a variant of naive learning from Friedkin and Johnsen (1999). Instead of assuming a constant prior, we assume it to be updated each period.

$$\tilde{\psi}_{i,t} = (1 - \lambda)\hat{\psi}_{i,t} + \lambda \sum_{j=1}^N w_{i,j} \tilde{\psi}_{j,t-1} \quad (3)$$

The belief $\hat{\psi}_{i,t}$ from the private learning is a weighted average of prior $\tilde{\psi}_{i,t-1}$ and an individual noisy signal, $s_{i,t}$, where a constant weight k is given to new signals.

$$\hat{\psi}_{i,t} = (1 - k)\tilde{\psi}_{i,t-1} + ks_{i,t} \quad (4)$$

This formulation nests various expectation formation mechanisms developed in the literature, including information rigidity due to noisy information (in the form of Kalman filtering, (Coibion and Gorodnichenko, 2015a)), and overreaction due to “diagnostic expectations” (Bordalo et al., 2020). Generally, k can be time varying and optimally adjusted based on the noisiness of signals, as assumed in the original Kalman filtering. We focus on the case of a constant k for realism.

Combining private and social learning defined above gives a linear recursive formula expressed only in terms of post-communication belief $\tilde{\psi}_{i,t}$.

$$\tilde{\psi}_{i,t} = (1 - \lambda)(1 - k)\tilde{\psi}_{i,t-1} + \lambda \sum_{i=1}^N w_{i,j} \tilde{\psi}_{j,t-1} + (1 - \lambda)ks_{i,t} \quad (5)$$

It is worth commenting on why such a form of social learning is “naive”. When agents repeatedly take the average of the posteriors of their connected nodes using the constant weight, they fail to account for possible repetition in the information contained in others’ signals as if they are independent signals. This heuristic rule is justified by assuming agents do not have perfect knowledge of the whole network structure and cannot trace the source of information received from friends due

to bounded rationality (Chandrasekhar et al., 2020). Instead of optimally adjusting the weights to each signal based on their precision, each person simply uses the same weights from social connectedness. This gives rise to the “persuasion bias” shown in DeMarzo et al. (2003). It states that the consensus that arises after repeated communications among agents do not converge to the correct belief unless the social influence structure is balanced. The model also implies persistent differences in opinions in the presence of heterogeneous priors, and the speed of belief convergence is slower than in a rational framework where agents optimally adjust weights given the precision of signals.¹⁶

We also characterize the belief dynamics for the entire society. Stacking individual beliefs into a N -sized vector $\tilde{\psi}_t$ each period after social learning, the belief dynamics can be summarized by the following.

$$\begin{aligned}\tilde{\psi}_t &= M\tilde{\psi}_{t-1} + (1 - \lambda)ks_t \\ M &= (1 - \lambda)(1 - k)I + \lambda W\end{aligned}\tag{6}$$

where s_t is a $N \times 1$ vector stacking all individual signals at t and κ_t is a $N \times N$ matrix with its i -th diagonal element being the agent i 's information gain and zeros elsewhere. I is an identity matrix sized N . The weight assigned to the previous belief M consists of one component from individual updating and another from social communication determined by the network structure W (given $\lambda > 0$).

4.2 Implications for Shock Propagation

Regardless of the specific form of individual learning (various values of k), the presence of social communication ($\lambda > 0$) introduces a mechanism via which idiosyncratic shocks that hit a certain

¹⁶See this [Jupyter Notebook](#) for the simulation exercises of these results using SCI data.

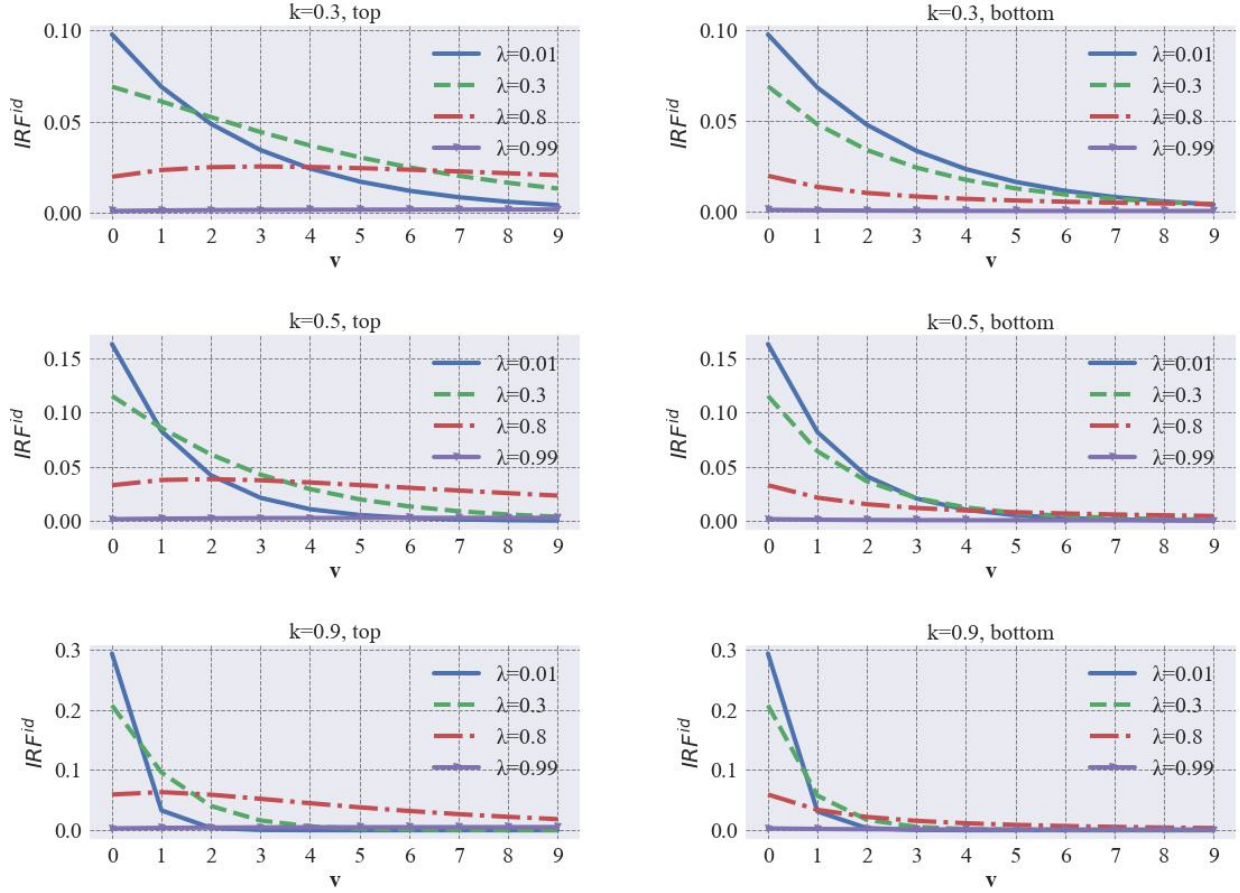
fraction of the agents can propagate into the society level through its effects on the distribution of the beliefs regarding $\tilde{\psi}$. This is particularly relevant when the listening matrix is more asymmetric, and when more influential nodes are hit by the idiosyncratic shocks. Figure 2 illustrates these points by showing the impulse responses of the average belief, $\tilde{\psi}^{av}$, to a one-time and equally sized shock to the beliefs ($\tilde{\psi}_i$) of the top (left panel) and bottom (right panel) one-third of agents in terms of their influence, under a range of values of k and λ . We use the listening matrix from SCI in 2019 as the input, although the patterns hold for any asymmetric matrix.

In period $v = 0$, the initial response is equal to $\frac{1}{3}(1 - \lambda)k$ across different parameter values. The subsequent path of the response exhibits different patterns; it is not always monotonic. Although ultimately the local news is moderated in social communication, and the society's belief responses converge to zero because the shocks are idiosyncratic by assumption and are exogenous to the underlying aggregate state, the aggregate belief may exhibit a hump-shaped adjustment if social communication has a relatively high weight (larger λ) and individual responsiveness is moderate (small k). A higher social weight and lower responsiveness to the news allows the noise to slowly unfold and spread through the network before being diluted away. This can be seen in the IRFs with $\lambda = 0.8$, where the idiosyncratic shocks have long-lasting effects on aggregate beliefs.

Lastly, the left and right panels in Figure 2 also show noticeable differences in the paths of shock propagation depending on whether the top or bottom influencers are hit. Since the local shocks that hit the bottom influencers are not amplified to the society as those hitting the top influencers from the beginning, the response only has a one-time jump and then gradually subsides afterward. The difference is also smallest when the role of social communication is less significant (small λ).

Another determinant of the belief dynamics is the structure of the listening matrix. The most relevant structural property is the distribution of degrees across agents. For all balanced or symmetric listening matrices with zero dispersion (every node has a degree of 1), the structure of the

Figure 2: Impulse Responses of the Average Belief $\tilde{\psi}_{t+v}^{av}$ to Local News Shocks



Note: This figure plots, under various parameter values of λ and k , the impulse responses of the average belief $\tilde{\psi}^{av}$ in v periods after a local news shock to the top (left) and bottom (right) one-third fraction of nodes at $t = 0$.

network and the location of the shocks is no longer relevant to the transmission of local shocks to aggregate beliefs. An asymmetric matrix with a higher degree of dispersion implies more asymmetric influences among agents, and local shocks to nodes of different influences would now have disproportionate impacts on aggregate belief and its dynamics.

5 A Quantitative Model of Consumption in the Pandemic

This section builds the network-based learning framework formulated in Section 4 into a pandemic-augmented consumption and saving model with uninsured idiosyncratic income risks and borrowing

constraints. We explore whether the effect of social influences on individual expectations and consumption spending generates a sizable aggregate response that alters the macroeconomic dynamics.

We allow for two consumption sectors that are potentially affected differently by the pandemic. Moreover, given our primary focus is the propagation mechanisms of aggregate demand via social networks, we adopt a partial equilibrium approach by taking the supply side of the economy as given. However, nominal rigidity and cross-sector frictions could be added to a general equilibrium model so that the aggregate demand generates real effects in output and unemployment.

It should be noted that our choice of specifically modeling the pandemic environment was meant to be more comparable to our reduced-form empirical evidence. We explore aggregate implications of the social communication mechanisms in a more general setting in a companion ongoing project.

5.1 The Consumer's Problem

The economy is populated by N infinitely-lived consumers, indexed by i . Each consumer derives utility from a stream of consumption in the current and all future periods.

$$\max E_0 \sum_{t=0}^{\infty} \beta^t u(c_{i,t}) \quad (7)$$

The instantaneous utility within each period takes a CRRA form with relative risk aversion ρ (and the elasticity of intertemporal substitution $\frac{1}{\rho}$).

$$u(c) = \frac{c^{1-\rho}}{1-\rho} \quad (8)$$

Total consumption in each period, denoted as c_t , is a CES (constant elasticity of substitution) bundle of goods/services from two sectors: one contact-based represented by subscript c and non-contact-based consumption by n , respectively.

$$c_{i,t} = (\tau_{i,t}\phi_c c_{i,c,t}^{\frac{\epsilon-1}{\epsilon}} + (1-\phi_c)c_{i,n,t}^{\frac{\epsilon-1}{\epsilon}})^{\frac{\epsilon}{\epsilon-1}} \quad (9)$$

The elasticity of substitution between two sectors is ϵ and the relative preference weight are ϕ_c and $1 - \phi_c$: a larger ϵ implies the two sectors are more substitutable and a larger ϕ_c implies a stronger relative preference toward contact-based consumption. Moreover, the taste shock, denoted as $\tau_{i,t}$, scales the utility from contact-based consumption. In the steady state, it takes a value of 1.

In each period t , the agent receives an idiosyncratic draw of the taste shock, $\tau_{i,t}$, which varies with the local infections, and this is specified later. Lower $\tau_{i,t}$ implies less utility from consuming contact-based services due to exposure to infection. This conveniently captures the idea that consuming contact-consumption bears higher health risks from the individual's point of view. A lower utility from contact-based consumption could be either due to self-precautionary actions to avoid infection or compliance with local government containment policies such as stay-at-home orders.

The intertemporal budget and borrowing constraints of the agent i at time t are the following.

$$\begin{aligned} c_{i,t} + a_{i,t} &= m_{i,t} \\ m_{i,t} &= y_{i,t} + b_{i,t} \\ b_{i,t+1} &= a_{i,t}(1+r) \\ a_{i,t} &\geq 0 \end{aligned} \quad (10)$$

where $a_{i,t}$ is the end-of-period saving at a real interest rate r , $m_{i,t}$ is the total wealth in hand, consisting of the current bank balance $b_{i,t}$ and the labor income $y_{i,t}$, which is determined by.

$$\begin{aligned}
y_{i,t} &= n_{i,t} o_{i,t} z_{i,t} \\
\log(o_{i,t}) &= \log(o_{i,t-1}) + v_{i,t} \\
v_{i,t} &\sim N\left(-\frac{\sigma_v^2}{2}, \sigma_v^2\right)
\end{aligned} \tag{11}$$

where $n_{i,t}$ is the labor supplied inelastically, which we normalize to one. The labor income received by an individual i depends on the realizations of two multiplicative idiosyncratic income shocks: a permanent component $o_{i,t}$, and a transitory (or a persistent) component $z_{i,t}$, which is potentially a function of local infection. The logged permanent income $o_{i,t}$ follows a random walk with i.i.d. shock of size σ_v .¹⁷ The component $z_{i,t}$ is equivalent to a standard transitory income component without the impact from the local infection. During the pandemic, a higher infection leads to lower income or unemployment. We specify $z_{i,t}$ as a function of infection later.

5.2 The Pandemic

We model the pandemic as an agent-specific stochastic state that evolves subject to both aggregate and idiosyncratic shocks. Each agent i at time t is faced with a local infection state, $\Xi_{i,t}$, which represents the severity of the local epidemic. It could be approximated, for example, by the reported COVID infections in the region. $\Xi_{i,t}$ grows exponentially with two multiplicative components: one an aggregate growth rate of $\exp(\psi_t)$, and the other an idiosyncratic shock $\exp(\eta_{i,t})$. The combined growth rate from the two shocks is equivalent to what is commonly referred to as the “reproduction rate” in a micro-founded epidemiological model such as SIR or SIRD.¹⁸ The aggregate state follows a random walk. Both aggregate shock, θ_t , and idiosyncratic shock, $\eta_{i,t}$, are log-normally distributed

¹⁷We set its mean to be $-\sigma_v^2/2$ so that the expected value of $o_{i,t}$ is unity. This follows from the fact that for a random variable $x \sim N(\mu, \sigma^2)$, the expectation of its exponential $E(\exp(x)) = \exp(\mu + \sigma^2)$

¹⁸For instance, see Eichenbaum et al. (2021) and Krueger et al. (2022).

with mean zeros. Taking the log, we obtain a law of motion of local infection.

$$\begin{aligned}\Xi_{i,t} &= \exp(\psi_t) \exp(\eta_{i,t}) \Xi_{i,t-1} \\ \log(\Xi_{i,t}) &\equiv \xi_{i,t} = \psi_t + \eta_{i,t} + \xi_{i,t-1} \\ \psi_t &= \psi_{t-1} + \theta_t\end{aligned}\tag{12}$$

Our main assumption is that agents do not have perfect observation of the aggregate transmission ψ_t in real time. Instead, they form subjective perceptions about it $\tilde{\psi}_{i,t}$ following the learning rule defined in Section 4. In the individual updating, the observed changes in local infections are used as the noisy signals, which consist of the true state ψ_t and noises $\eta_{i,t}$. Under these specific assumptions, the aggregate shock θ_t in this model is a fundamentally relevant and permanent shock for learning. The local shock is from idiosyncratic changes in infections, which are time-independent noises for belief updating. It instead affects the consumption of individual agents directly.

$$s_{i,t} = \xi_{i,t} - \xi_{i,t-1} = \psi_t + \eta_{i,t}\tag{13}$$

The local infection state $\xi_{i,t}$ affects the time-varying taste shock $\tau_{i,t}$ and individual productivity shock $z_{i,t}$ according to the following linear functions.

$$\begin{aligned}\log(\tau_{i,t}) &= \alpha_s \xi_{i,t} + \mu_{i,t} \\ \log(z_{i,t}) &= \alpha_z \xi_{i,t} + \zeta_{i,t} \\ \mu_{i,t} &\sim N(-\frac{\sigma_\mu^2}{2}, \sigma_\mu^2) \\ \zeta_{i,t} &\sim N(-\frac{\sigma_\zeta^2}{2}, \sigma_\zeta^2)\end{aligned}\tag{14}$$

Logged preference $\tau_{i,t}$ and labor productivity $z_{i,t}$ are both linear functions of the underlying infection state $\xi_{i,t}$ plus i.i.d. shocks $\mu_{i,t}$ and $\zeta_{i,t}$, respectively. Both shocks are normally distributed with standard deviations of σ_μ and σ_ζ .¹⁹ α_s and α_z are the loading parameters from the infection to preference and individual income, respectively. Since higher infections cause income to drop. and increases the disutility from contact-based consumption, both α_s and α_z are negative by assumption.

5.3 Optimal Consumption

We start by characterizing the optimal consumption policy and sector-specific demand function of the individual consumer. Under perfect understanding of the spreading speed of the virus, an individual's optimal consumption depends on local infection $\xi_{i,t}$ together with preference weight $\tau_{i,t}$, wealth in hand $m_{i,t}$ and permanent income $o_{i,t}$. Under the “learning from friends”, the perceived state of infectiousness $\tilde{\psi}_{i,t}$ enters as an additional state variable. An individual's value function at time t is therefore evaluated based on her perceived state of the world, $\tilde{\psi}_{i,t}$, the local infection $\xi_{i,t}$, the draw of the taste weight $\tau_{i,t}$ in addition to permanent income $o_{i,t}$ and total wealth $m_{i,t}$.

$$V_{i,t}(m_{i,t}, o_{i,t}, \tilde{\psi}_{i,t}, \xi_{i,t}, \tau_{i,t}) = \max_{\{c_{i,c,t}, c_{i,n,t}\}} u(c_{i,t}(c_{i,c,t}, c_{i,n,t})) + \beta \tilde{E}_{i,t} V_{i,t+1}(m_{i,t+1}, o_{i,t+1}, \psi_{t+1}, \xi_{i,t+1}, \tau_{i,t+1}) \quad (15)$$

Notice that the expected value in the above value function is evaluated on the individual-time specific expectation operator, $\tilde{E}_{i,t}()$. Each agent uses her perceived aggregate state $\tilde{\psi}_{i,t}$ at time t to infer the aggregate state ψ_{t+1} in the next period. Following the common practice in many dynamic decision models involving belief updating, we adopt the bounded rationality assumption, i.e. individuals ignore the possibility of future belief updating when evaluating the expected value

¹⁹Their means are both adjusted so that the expected value of $\exp(\mu_{i,t})$ and $\exp(\zeta_{i,t})$ are equal to one.

of their actions. This explains why we write ψ_{t+1} instead of $\tilde{\psi}_{i,t+1}$ within the expectation operator.

Further simplification of the problem can be made, since the value function treats the choices in intertemporal consumption policy and sector-specific demand as one problem. It turns out that we can separately solve the two problems to reduce the number of state variables. This is due to the two-stage budgeting principle. Since the CES aggregator within the period is homothetic, the indirect utility gained within each period from an optimal allocation between two sectors becomes independent from the realization of the preference shock. We can first solve the intertemporal problem by treating the total consumption as the single control variable. The value function associated with the problem can be written as the following.

$$V_{i,t}(m_{i,t}, o_{i,t}, \tilde{\psi}_{i,t}, \xi_{i,t}) = \max_{\{c_{i,t}\}} u(c_{i,t}) + \beta \tilde{E}_{i,t} V_{i,t+1}(m_{i,t+1}, o_{i,t+1}, \psi_{i,t+1}, \xi_{i,t+1}) \quad (16)$$

Applying the Envelope Theorem to the value function, we can obtain the households' Euler equation associated with the total consumption $c_{i,t}$ as the following.²⁰

$$\tilde{E}_{i,t}[e^{(1-\rho)v_{i,t+1}} u'_{t+1}(\frac{c_{i,t+1}}{o_{i,t+1}})] = \beta(1+r)u'_t(\frac{c_{i,t}}{o_{i,t}}) \quad (17)$$

Intertemporal optimality requires proportional allocation between c and n depending on the taste shifter $\tau_{i,t}$. It is solved as an allocation of the total consumption into two categories based on the realized preference and the relative price of the two. We assume the relative nominal price of the two is one.

²⁰When solving optimal consumption in the presence of permanent income, one commonly used trick is to normalize consumption and asset by the permanent income level to reduce the number of state variables by 1. We do the same following Gourinchas and Parker (2002) and Carroll (2011).

$$\frac{u_{c_c}(c_{i,c,t}, c_{i,n,t})}{u_{c_n}(c_{i,c,t}, c_{i,n,t})} = \frac{\tau_{i,t}\phi_c}{1-\phi_c} \left(\frac{c_{i,c,t}}{c_{i,n,t}}\right)^{-\frac{1}{\epsilon}} = 1 \quad (18)$$

5.4 Parameter Calibration

The two structural parameters in the model regard belief formation: λ and k . A direct identification of these two parameters requires individual panel data of beliefs in addition to an SCI-based listening matrix, a task to which we decided to devote a separate paper. Instead, we indirectly calibrate the two parameters based on empirically recovered consumption responses to infection shocks. That is, the individual consumption response to local infections is equal to the multiplicative term $a_z k(1-\lambda)$, according to Equation 5 and the convenient fact in this model that consumption is a linear function of the individual belief $\tilde{\psi}_{i,t}$ scaled by the income elasticity to infections a_z .

In particular, we choose the combination of k and λ such that the sensitivity of consumption with respect to contemporaneous local infections is 0.015, the baseline estimated coefficient from Table 1. Dividing it by a value of α_z , say 0.1, gives exactly the consumption-implied belief sensitivity of $(1 - \lambda)k = 0.15$. At the same time, we know that cross-sectional variations in consumption sensitivity to differently socially weighted shocks reveal the value of λ independent of k .

What is a reasonable value of α_z ? Due to limited access to high-frequency cross-sectional income data, we choose not to estimate it externally. More importantly, we believe that the assumed loading from infection to the income, in reality, is just a catch-all parameter that embeds various channels perceived by households, such as drops in consumer expectations (Eichenbaum et al., 2022) and the introduction of nonpharmaceutical interventions (NPIs) (Coibion et al., 2020b), particularly on hospitality, arts, and leisure sectors (Huang et al., 2020). Hence, we choose a baseline value of 0.1, meaning that a 1% percentage increase in local infection leads to a 0.1% drop in income, which we

view as an extremely conservative estimate and invite further research over.²¹

We set the loading parameter of the infection to the preference α_s to be -0.2 to match an upper-bound value of the estimated elasticity of contact-based spending to local cases of 0.05% reported in the Figure A.1. This is set to be internally consistent with the chosen value of $\alpha_z = -0.1$, which reflects a higher dis-utility of contact-based consumption and guarantees that $\tau_{i,t} < 1$, i.e., infection lowers the weight of the contact sector compared to its steady-state level. Finally, the size of taste shock $\sigma_\mu = 2.9$ is chosen to match the cross-sectional inequality of contact/non-contact-based consumption before the pandemic, as we discuss along Figure 3.

We estimate the parameters of the infection dynamics as described by Equation 12 using the weekly panel of reported cases of U.S. counties between Feb 1st to June 30th. The estimation takes a form of GMM. We first take the double difference of log infections to get the sample analogue of $\theta_t + \eta_{i,t}$. Then a time-fixed effect regression on this residual will decompose the shock into an aggregate and idiosyncratic component. Taking the cross-sample standard-deviation of the time-fixed effects and the residuals gives the estimates for $\sigma_\theta = 0.1209$ and $\sigma_\eta = 0.209$, respectively.

Besides, one of the novel additions of this model regards the distinction between two sectors of consumption that bear different infection risk. The literature has not provided an estimate regarding the preference parameters associated with the subcategory demand. We therefore rely upon both Consumer Expenditure Survey (CEX) and the card transaction data to infer them. We group reported subcategory consumption series into contact and non-contact-based ones. The steady-state share of contact consumption ϕ_c is then set to be 0.41.

We also estimate the elasticity of substitution (EOS) between the two via a reduced-form regres-

²¹In fact, the recent survey evidence by Dietrich et al. (2022) shows that average U.S. households expected a drop of 15% in GDP and 13% in their own household income in middle March 2022, where the total number of infected cases remained in two digits. The perceived COVID-19 income effects by households were drastic and large. See Coibion et al. (2020b) for additional evidence of consumer expectations about COVID-19 and their corresponding economic forecasts.

sion of the change in one on that of the other. Our estimates suggest an ϵ of 0.75. This indicates that our baseline model assumes the two sectors of consumption are gross complements. We recognize the substantial disagreement on the assumption regarding the substitutability of the two sectors in the recent literature about the pandemic. For instance, Krueger et al. (2022) assumes a baseline EOS of 3 and 11 for the alternative assumptions, although no empirical estimates are provided. Guerrieri et al. (2020) discusses the important aggregate demand implications of the value of EOS without taking an empirical stance on it. Given this, we will compare the calibration results by assuming complementarity and substitutability in later sections.

The non-pandemic block of parameters of income process and preferences is standard. The size of permanent income volatility σ_v^2 is set to be $0.01 * 4/11$. The size of transitory income volatility σ_ζ^2 is set to be $0.01 * 4$, both of which are quarterly counterparts of annual volatility commonly used in the literature. This allows us to match the cross-sectional consumption inequality during the run-up of the pandemic (see Figure 3). For our other preference parameters, we follow the standard consumption/saving literature in choosing the preference parameters. Since the model is set at a quarterly frequency, both the time discount factor and interest rates are converted accordingly: $\beta = 0.99^{1/4}$ and $1 + r = 1.02^{1/4}$. The relative risk aversion ρ is 2.

The exact procedures of calibration are as followed. (1) Solve the model based on the optimality conditions laid out in the previous section. (2) Simulate the cross-sectional histories of idiosyncratic infections and the corresponding perceptions of individual agents about the aggregate state using the belief updating rule in this paper. (3) Simulate the history of individual consumption streams based on the simulated beliefs and resulting assets, and compute the aggregate consumption responses.

6 Counterfactual Experiments

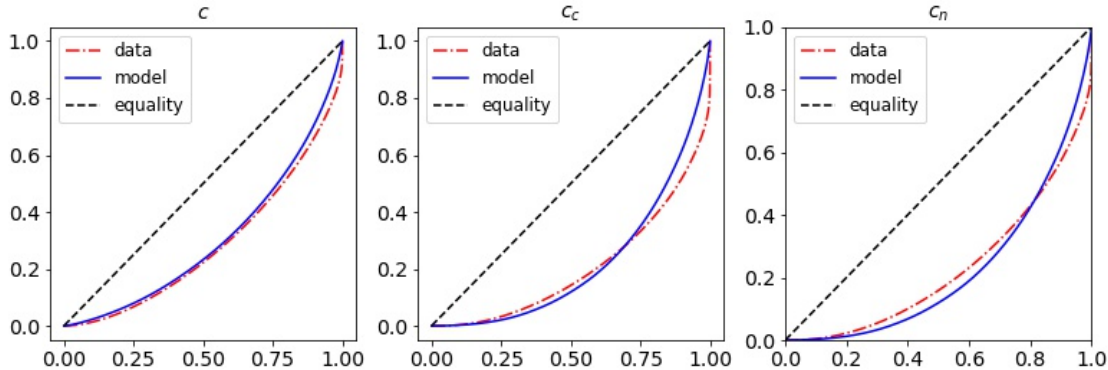
6.1 Benchmark: Pre-pandemic Consumption

Before exploring the implications of the pandemic for the consumption responses, we first calibrate the model for the pre-pandemic period. Specifically, we set the underlying local infection state to be zero $\xi_{i,t} = 0$ deterministically for all agents in the economy. This turns the income process into a standard permanent/transitory two-component process. The relative preference for contact versus non-contact consumption now depends solely on the idiosyncratic and transitory taste shock.

Like many other models featuring ex-ante homogeneity and uninsured idiosyncratic income risks (Castaneda et al., 2003; Carroll et al., 2017), our model generates ex-post heterogeneity across agents in terms of consumption and wealth. Since the data on cross-county wealth is not available, we focus on consumption inequality. We simulate the pre-pandemic histories of the economy for a long period of time such that the cross-sectional consumption inequality implied from the simulation broadly matches that from the data, giving us a useful benchmark.

Figure 3 plots the simulated and data-implied Lorenz Curves of total and subcategory consumption across all U.S. counties in our data sample before the pandemic. Since we suspect that the inequality suggested by the raw transaction data is driven by cross-regional differences in the data coverage and other unobservable characteristics, we compute the consumption inequality based on regression residuals of the consumer spending on a broad set of county-specific variables, including population, GDP per capita, the share of males, the education distribution, and the race distribution. This implies a cross-sectional standard deviation of log consumption per capita of 0.89 over the period of June 2017 to February 2020. While it is larger than the 0.3 to 0.45 dispersion of log consumption found in other household data, our calibrated parameters nonetheless allow us to broadly match the consumption inequality (Blundell et al., 2008; Heathcote et al., 2010; Kaplan and Violante, 2010; Heathcote et al., 2014; Aguiar and Bils, 2015).

Figure 3: Lorenz Curve of Cross-county Consumption Before the Pandemic



Note: This plot compares the Lorenz Curves of consumption across counties computed from data and simulated from the model. Consumption from data is based on the regression residuals of county-level spending on a list of county-specific demographics. Average consumption between January and February 2020 is used.

We can also validate the assumption of the model regarding the two sectors by examining the subcategory consumption inequality. We group detailed card spending data into two sectors, as we defined in this paper. Lorenz Curves of contact and non-contact-based consumption, which are shown in the middle and right panel in Figure 3 indicate that the consumption inequality within categories is higher than the total consumption, suggesting the role of heterogeneity in preference shocks. This subcategory inequality helps identify the size of preference shock $\sigma_\tau = 2.9$. We pick this value such that the Lorenz Curves of both categories match that from data, respectively (e.g., Aguiar and Hurst (2013) and Attanasio and Pistaferri (2016)).

Taking the pre-pandemic wealth distribution as the initial condition, we proceed to explore the aggregate consumption responses after the outbreak of the pandemic. At the time $t = 0$, we hit a chosen fraction of agents with an infection shock to get the impulse responses of the economy. All impulse responses are defined as the differences between shocked paths of aggregate variables relative to the steady-state scenario where there is no change in infections in all nodes. We also assume that all agents start with a common and correct prior about the aggregate transmission rates. At the same time, individuals keep drawing new permanent and transitory income shocks.

6.2 Experiment 1: Different Degrees of Social Communication

We first examine the aggregate responses under imperfect information regarding aggregate transmission with different degrees of social communication (different λ s). $\lambda = 0$ corresponds to the case of zero-social communication. We undertake the analysis fixing the degree of individual responsiveness k at $\kappa^* = 0.33$, the steady-state weight from Kalman filtering computed from estimated volatility of aggregate and local infections (see Appendix A.5 for derivations). This is essentially to assume individuals rationally respond to their local news under imperfect information. Furthermore, the shock is assumed to hit the top one-third of nodes according to the influence.

Figure 4 shows the responses of aggregate variables. A 10% increase in infections for a third of the agents corresponds to a 3.3% increase in the average infection in the economy and affects the average wealth via the income shocks correspondingly. The aggregate belief overreacts compared to the full-information case since by assumption of the experiment the shocks are local and did not alter the spreading speed of the virus.

With social communication, the same news will be propagated to the economy along different paths depending on the degree of communication, thus inducing different aggregate consumption responses. A bigger value of λ lowers the initial response to the shock but slows the convergence speed to zero. The L-shaped belief responses under a lower social weight induce a bigger drop in consumption spending at first and are followed by a faster recovery afterward. In contrast, a moderate hump shape of belief response under more social communication smooths the responses to noises, hence the consumption dynamics. This suggests one of the possible drivers of different recovery patterns might be the effect of dispersed shocks from the COVID-19 surge on social networks

that in turn affect individual beliefs (Bailey et al., 2018a, 2022b).²²

Quantitatively speaking, moving from zero social communication to a medium level of social communication ($\lambda = 0.5$) implies a smaller drop in spending by 0.1 percentage points in the first period of the shock. The effects on sub-category consumption follow the same token, as higher perceived transmission not only lowers total consumption but also induces shifting toward non-contact consumption. Again, this is under the assumption that the income elasticity with respect to local infection is 0.1. A higher value implies a bigger difference in adjustments.

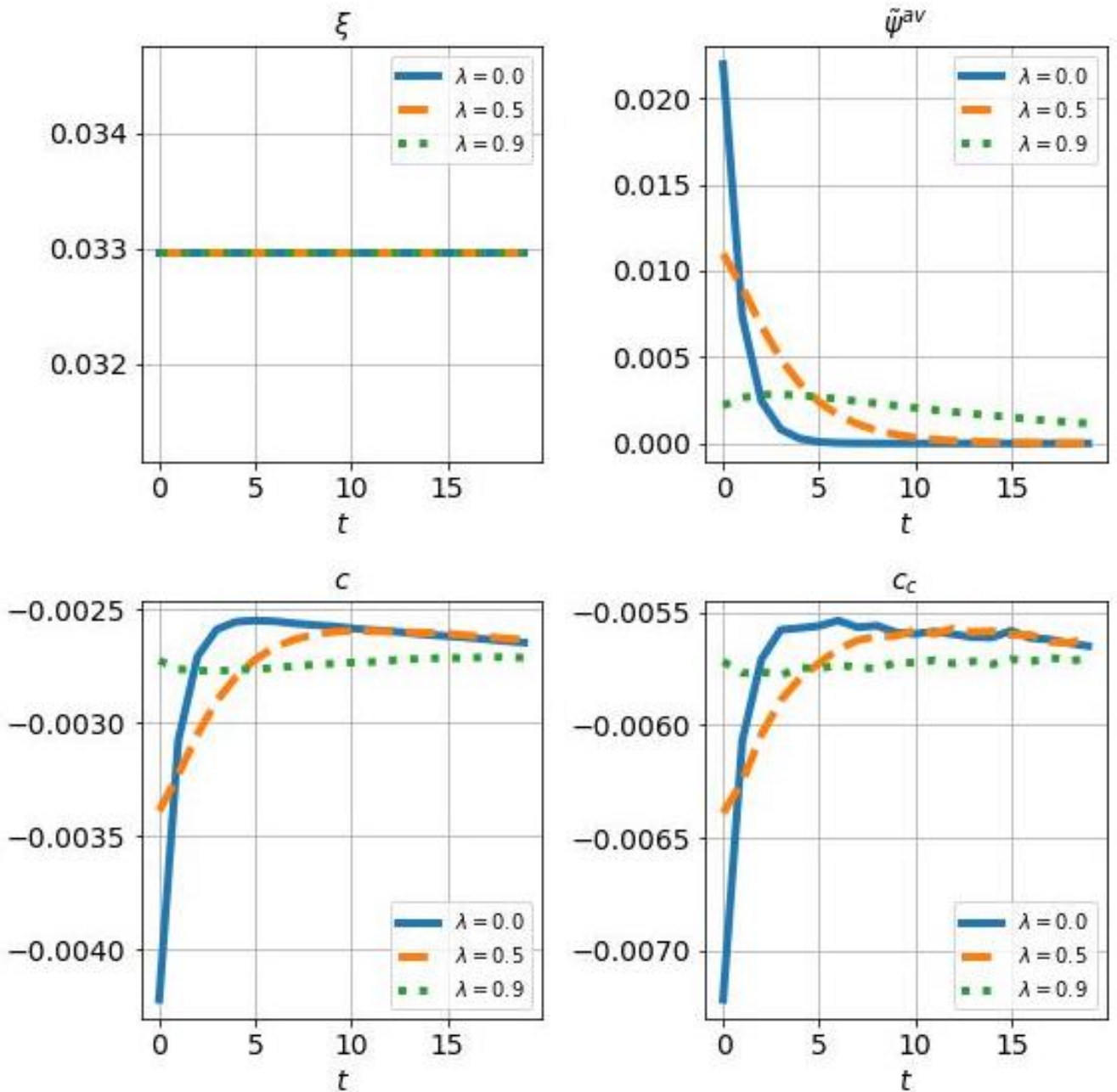
6.3 Experiment 2: The Location of the Pandemic Shock

Individual nodes have different influences in the network. Therefore, the aggregate responses may differ depending on where the infection shock takes place. Figure 5 plots the impulse response graphs following the same-sized 10% infection increase in the top, middle, and bottom one-third of the nodes in terms of their social influence measured by their degrees. It is not surprising that aggregate consumption sees the biggest reaction if the infection news takes place in the most influential agents in the economy. Although in all scenarios the initial drop in consumption is equal in size before the social communication, the shocks that hit the top influencers are first amplified via social communications thus inducing a further drop in aggregate consumption before the recovery while the other two scenarios see a gradual recovery following the initial shock. This suggests that the location of the initial shocks may not only affect the overall size of the aggregate demand response but also the shape of the dynamics.

This location-dependent mechanism of aggregate amplification is very similar in flavor to related macroeconomic work in other contexts such as input-output linkages (Acemoglu et al., 2012; vom Lehn and Winberry, 2020), but the impacts here are belief-driven. As our empirical evidence has

²²See Kuchler et al. (2023) for a survey on housing market expectations.

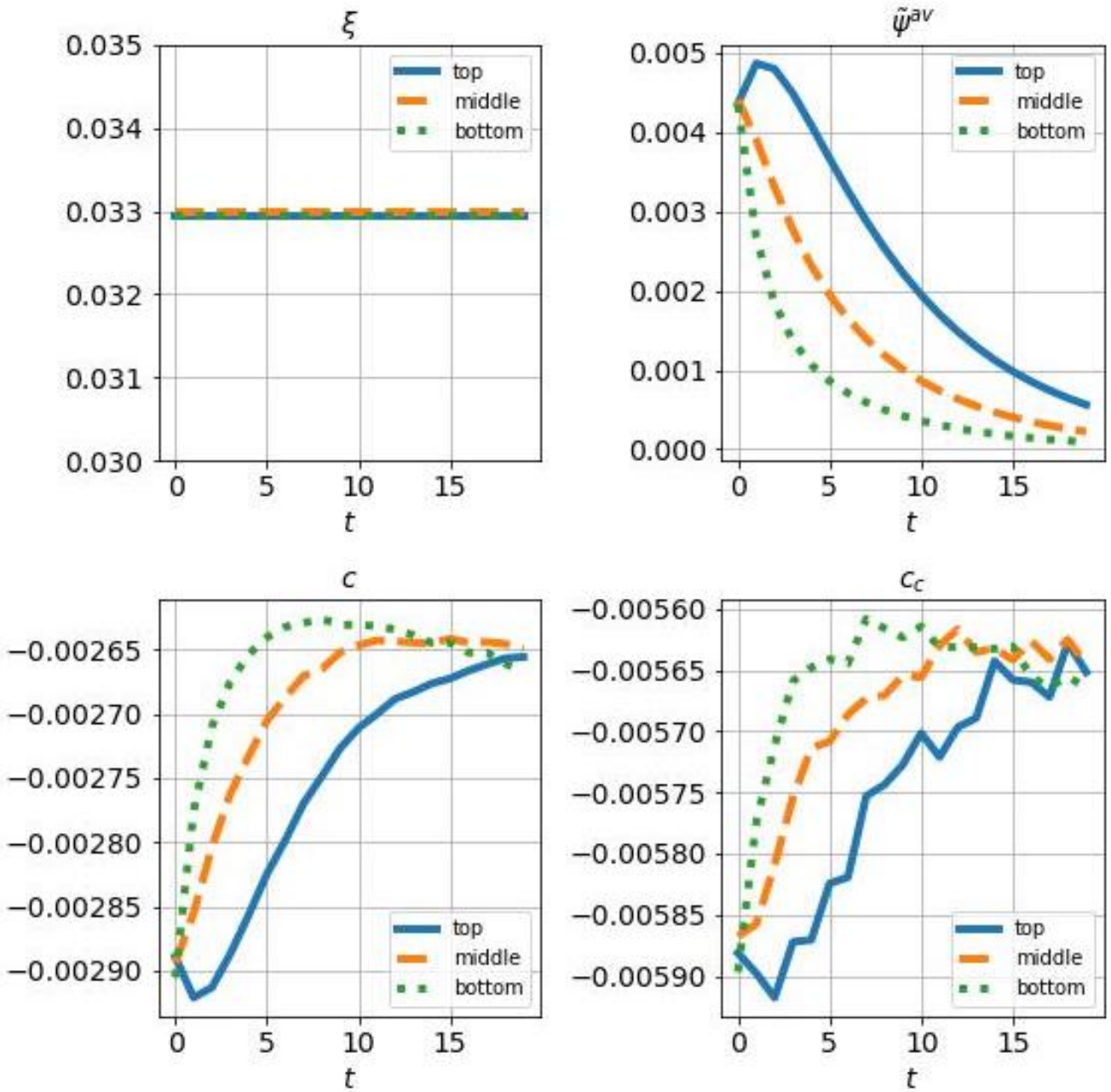
Figure 4: Impulse Responses of the Economy to An Infection Shock at Different Degrees of Social Communication



Note: This figure compares the impulse responses of the economy under different degrees of social communication (λ) following a 10% increase in one-third of the agents in the economy whose average degree is greater than 1 at time $t = 0$. The variables are average local infection ξ , average perceived transmission $\tilde{\psi}^{av}$, average total consumption c and average contact-based consumption c_c .

shown, a similar mechanism is present with the COVID-19 pandemic: since the infections first hit the metropolitan and well-connected regions such as New York City and Seattle, it is fair to conjecture that this has induced a more sizable drop in aggregate consumption than a counterfactual

Figure 5: Impulse Responses of the Economy to An Infection Shock in Nodes of Different Influences



Note: This figure compares the impulse responses of the economy following a 10% increase in a random top/middle/bottom third fraction of the most influential agents in the economy at time $t = 0$. The variables are average local infection ξ , average perceived transmission $\tilde{\psi}^{av}$, average total consumption c and average contact-based consumption c_c .

scenario where the COVID-19 first hitless connected regions.

6.4 Experiment 3: Alternative Network Structure

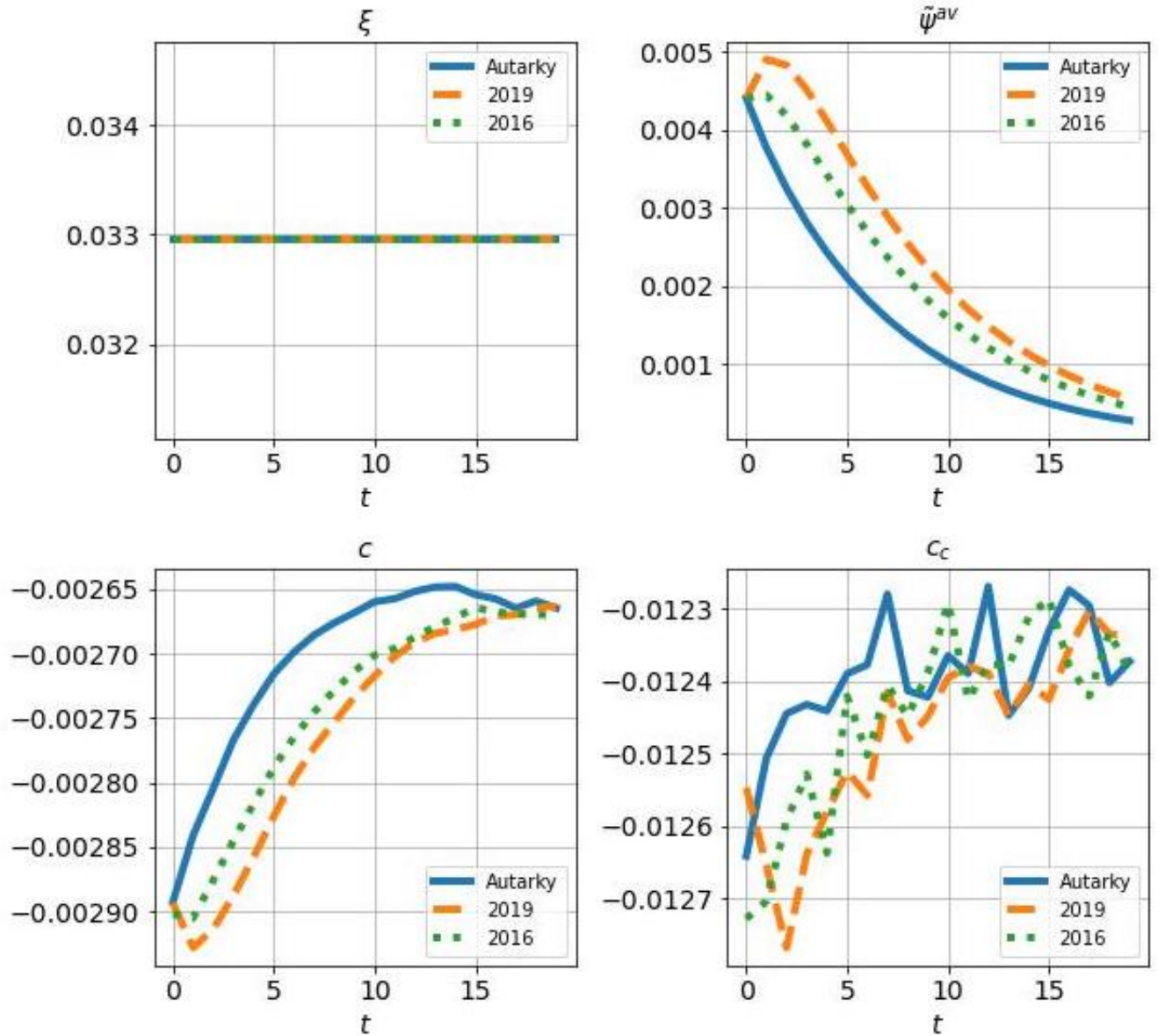
What would have happened to the consumption responses if the economy is set in a social network of different structures? Figure 6 compares the impulse responses to the same shock based on the social network in 2016, 2019, and an imagined autarky world, respectively. Since Figure A.7 shows that the social influence has grown more dispersed over time, shocks that take place in the most influential nodes will receive greater weight. This gives more room for possible amplification of the local shock via the network. Since the network does not affect the initial response, average belief responses are the same at the time of the shock but play out along different paths.

We set $\lambda = 0.7$ a larger value than our benchmark to show the differences from the network more clearly. Individual responsiveness k remains $\kappa^* = 0.33$. As the Figure shows, the belief response in 2016 no longer takes a hump pattern as in 2019 due to the smaller dispersion in influence. An autarky network, not surprisingly, shows a rapid return to zero following the shock due to zero influence from others. Despite the differences in belief patterns, their implied differences in consumption spending end up being negligible in this scenario. All three scenarios witness around a same-sized drop of 0.5% and almost identical consumption recovery following the shock.

Of course, for higher sensitivity of income to the infection or more overreaction to the news at the individual level, the differences in the macroeconomic impacts by different networks will be more significant. We take this evidence as assurance regarding our modeling assumption that the weight matrix is time-invariant. Our conjecture is that the slow-moving nature of the social networks at the macro level will not fundamentally change the macroeconomic responses. The results help confirm this. However, we remain cautious about overinterpreting these results because the alternative network structure could have a much higher dispersion in influences than the observable ones. It is nonetheless clear that a more asymmetric network will increase the chance that any local shocks,

especially those that hit the influential, contribute to aggregate effects.

Figure 6: Impulse Responses of the Economy to An Infection Shock: Different Social Networks



Note: This figure compares the impulse responses of the economy following a 10% increase in the top one third most influential nodes in the economy at time $t = 0$ under the social network in 2016 and 2019. The variables are average local infection ξ , average perceived local infection $\tilde{\psi}^{av}$, average total consumption c and average contact-based consumption c_c .

6.5 Discussion

Although our model is tailored towards understanding the quantitative effects of the pandemic on consumption, the framework is flexible, and it carries broader implications for how social networks

can have an aggregate effect in a more general macroeconomic setting. The core structure of the framework is that individual agents form beliefs about some unobservable aggregate state of the economy via private updating of noisy local signals and social communication. We show, in such an environment, the impacts of a higher degree of social communication also depend on individual responses to their own news. Higher social influence moderate beliefs swing by counterbalancing overreactions to noises. But this comes at the cost of slower learning at the society level. By this token, the welfare effects from higher social communication crucially depend on the nature of the shocks as well as the degree of the irrationality of individuals.

The presence of interpersonal influences on beliefs, hence resulting in interconnection in behaviors, poses an important question on how to think about the impacts of local/idiosyncratic shocks at the aggregate level. Due to asymmetric influences of different agents in the network, even independently drawn shocks across the economy induces non-balanced responses to the news at the aggregate level. The effect tends to be higher with more overreaction by individuals. Our paper suggests that acknowledging these effects is important when considering the macroeconomic effects of local shocks. This point is essentially very similar to the rapidly developing literature on the production networks and their macroeconomic effects (Acemoglu et al., 2012; Baqaee and Farhi, 2018), although our focus is on interpersonal influences via beliefs.

What this paper does not fully explore are the implications of social communication on belief heterogeneity and how it interacts with market incompleteness. On one hand, social learning induces more convergence in beliefs among individuals due to mutual influence, on the other hand, the slow-spreading nature of such an environment also leads to non-monotonic patterns of cross-sectional belief dispersion. Combined with ex-post heterogeneity in wealth and the marginal propensity to consume from uninsured income shocks, the cross-sectional consumption responses as well as its inequality properties will be different. We leave this for future work to explore.

7 Conclusion

How are economic behaviors such as consumption affected by social communication and information disseminated via online networks? What are their implications for macroeconomic shock propagation mechanisms? This paper tackles these questions both empirically and theoretically.

We first identify the effects of using 5.18 million debit card users' transactions across the United States during COVID-19 and large-scale online social networks. We found significant consumption adjustments in responses to the infection news in one's socially connected counties/foreign countries.

We then extend a standard incomplete-market model to a pandemic setting, featuring belief updating from both private signals and social communications. We show how social communication may moderate overreaction to irrelevant local news in the aggregation, but also slows down the belief adjustment to fundamentally relevant shocks. Our model also shows how shocks to different locations of the social network can amplify and propagate macroeconomic fluctuations, especially for consumption. Future research should incorporate microdata directly on beliefs linked with consumption and the social network so that the parameters governing the belief formation process can be estimated jointly and used to disentangle among different theories of belief formation.

References

- Acemoglu, D., Carvalho, V. M., Ozdaglar, A., and Tahbaz-Salehi, A. (2012). The network origins of aggregate fluctuations. *Econometrica*, 80(5):1977–2016.
- Acemoglu, D., Ozdaglar, A., and ParandehGheibi, A. (2010). Spread of (mis) information in social networks. *Games and Economic Behavior*, 70(2):194–227.
- Agarwal, S., Liu, C., and Souleles, N. S. (2007). The reaction of consumer spending and debt to tax

- rebates: Evidence from consumer credit data. *Journal of Political Economy*, 115(6):986–1019.
- Aguiar, M. and Bils, M. (2015). Has consumption inequality mirrored income inequality? *American Economic Review*, 105(9):2725–56.
- Aguiar, M. and Hurst, E. (2013). Deconstructing life cycle expenditure. *Journal of Political Economy*, 121(3):437–492.
- Ali, U., Herbst, C. M., and Makridis, C. A. (2021). The Impact of Covid-19 on the U.S. Child Care Market: Evidence from Stay-at-Home Orders. *Economics of Education Review*, 82.
- Attanasio, O. P. and Pistaferri, L. (2016). Consumption inequality. *Journal of Economic Perspectives*, 30(2):3–28.
- Bailey, M., Cao, R., Kuchler, T., and Stroebel, J. (2018a). The economic effects of social networks: Evidence from the housing market. *Journal of Political Economy*, 126(6):2224–2276.
- Bailey, M., Cao, R., Kuchler, T., Stroebel, J., and Wong, A. (2018b). Social connectedness: Measurement, determinants, and effects. *Journal of Economic Perspectives*, 32(3):259–280.
- Bailey, M., Davila, E., Kuchler, T., and Stroebel, J. (2019). House price beliefs and mortgage leverage choice. *Review of Economic Studies*, 86:2403–2452.
- Bailey, M., Johnston, D., Koenen, M., Kuchler, T., Russel, D., and Stroebel, J. (2022a). Social networks shape beliefs and behavior: Evidence from social distancing during the COVID-19 pandemic. *Journal of Political Economy: Microeconomics*.
- Bailey, M., Johnston, D., Kuchler, T., Stroebel, J., and Wong, A. (2022b). Peer Effects in Product Adoption. *American Economic Journal: Applied Economics*, 14(3):488–526.
- Baker, S. R., Bloom, N., Davis, S. J., and Terry, S. J. (2020a). COVID-induced economic uncertainty. *NBER working paper*.
- Baker, S. R., Farrokhnia, R. A., Meyer, S., Pagel, M., and Yannelis, C. (2020b). How Does Household Spending Respond to an Epidemic? Consumption During the 2020 COVID-19 Pandemic.

Working paper.

- Baqae, D. R. and Farhi, E. (2018). Macroeconomics with heterogeneous agents and input-output networks. Technical report, National Bureau of Economic Research.
- Bartik, A. W., Betrand, M., Lin, F., Rothstein, J., and Unrath, M. (2020). Labor market impacts of COVID-19 on hourly workers in small- and medium- size businesses: Four facts from HomeBase data. *Chicago Booth Rustandy Center, Working Paper*.
- Bayer, P., Mangum, K., and Roberts, J. W. (2021). Speculative fever: Investor contagion in the housing bubble. *American Economic Review*, 111(2):609–51.
- Binder, C. and Makridis, C. A. (2020). Stuck in the Seventies: Gas Prices and Macroeconomic Expectation. *Review of Economics & Statistics, R&R*.
- Blundell, R., Pistaferri, L., and Preston, I. (2008). Consumption inequality and partial insurance. *American Economic Review*, 98(5):1887–1921.
- Bordalo, P., Gennaioli, N., Ma, Y., and Shleifer, A. (2020). Overreaction in macroeconomic expectations. *American Economic Review*.
- Burnside, C., Eichenbaum, M., and Rebelo, S. (2016). Understanding booms and busts in housing markets. *Journal of Political Economy*, 124(4):1088–1147.
- Cajner, T., Crane, L., Decker, R. A., Grigsby, J., Hamins-Puertolas, A., Hurst, E., Kurz, C., and Yildirmaz, A. (2020). The U.S. labor market during the beginning of the pandemic recession. *BFI working paper*.
- Canes-Wrone, B., Rothwell, J. T., and Makridis, C. A. (2022). Partisanship and policy on an emerging issue: Mass and elite responses to covid-19 as the pandemic evolved. *SSRN working paper*.
- Carroll, C., Slacalek, J., Tokuoka, K., and White, M. N. (2017). The distribution of wealth and the marginal propensity to consume. *Quantitative Economics*, 8(3):977–1020.

- Carroll, C. and Wang, T. (2023). Epidemiological expectations. In *Handbook of Economic Expectations*, pages 779–806. Elsevier.
- Carroll, C. D. (2003). Macroeconomic Expectations of Households and Professional Forecasters. *Quarterly Journal of Economics*, 118(1):269–298.
- Carroll, C. D. (2011). Solution methods for microeconomic dynamic stochastic optimization problems. *World Wide Web*: <http://www.econ.jhu.edu/people/ccarroll/solvingmicrodsops.pdf>. (accessed August 30, 2011). Cited on, page 28.
- Carroll, C. D., Fuhrer, J. C., and Wilcox, D. W. (1994). Does consumer sentiment forecast household spending? If so, why? *American Economic Review*, 84(5):1397–1408.
- Castaneda, A., Diaz-Gimenez, J., and Rios-Rull, J.-V. (2003). Accounting for the us earnings and wealth inequality. *Journal of political economy*, 111(4):818–857.
- Chandrasekhar, A. G., Larreguy, H., and Xandri, J. P. (2020). Testing models of social learning on networks: Evidence from two experiments. *Econometrica*, 88(1):1–32.
- Charoenwong, B., Kwan, A., and Pursiainen, V. (2020). Social connections with COVID-19 affected areas increase compliance with mobility restrictions. *Working paper*.
- Chen, X., Hong, H., and Nekipelov, D. (2011). Nonlinear models of measurement errors. *Journal of Economic Literature*, 49(4):901–937.
- Chetty, R., Friedman, J. N., Hendren, N., Stepner, M., et al. (2020). How did covid-19 and stabilization policies affect spending and employment? a new real-time economic tracker based on private sector data. Technical report, National Bureau of Economic Research.
- Cogley, T. and Sargent, T. J. (2008). The market price of risk and the equity premium: A legacy of the Great Depression. *Journal of Monetary Economics*, 55(3):454–476.
- Coibion, O. and Gorodnichenko, Y. (2015a). Information rigidity and the expectations formation process: A simple framework and new facts. *American Economic Review*, 105(8):2644–78.

- Coibion, O. and Gorodnichenko, Y. (2015b). Information Rigidity and the Expectations Formation Process: A Simple Framework and New Facts. *American Economic Review*, 105(8):2644–2678.
- Coibion, O., Gorodnichenko, Y., and Weber, M. (2020a). Labor markets during the COVID-19 crisis: A preliminary view. *NBER working paper*.
- Coibion, O., Gorodnichenko, Y., and Weber, M. (2020b). The cost of the COVID-19 crisis: Lock-downs, macroeconomic expectations, and consumer spending. *NBER working paper*.
- DeGroot, M. H. (1974). Reaching a consensus. *Journal of the American Statistical Association*, 69(345):118–121.
- DeMarzo, P. M., Vayanos, D., and Zwiebel, J. (2003). Persuasion bias, social influence, and unidimensional opinions. *Quarterly Journal of Economics*, 118(3):909–968.
- Di Maggio, M., Kermani, A., Keys, B. J., Piskorski, T., Ramcharan, R., Seru, A., and Yao, V. (2017). Interest rate pass-through: Mortgage rates, household consumption, and voluntary deleveraging. *American Economic Review*, 107(11):3550–3588.
- Dietrich, A. M., Kuester, K., Müller, G. J., and Schoenle, R. (2022). News and uncertainty about covid-19: Survey evidence and short-run economic impact. *Journal of monetary economics*.
- Dingel, J. I. and Neiman, B. (2020). How many jobs can be done at home. *BFI working paper*.
- Eichenbaum, M., de Matos, M. G., Lima, F., Rebelo, S., and Trabandt, M. (2022). Expectations, infections, and economic activity. *Working paper*.
- Eichenbaum, M., Rebelo, S., and Trabandt, M. (2021). The macroeconomics of epidemics. *Review of Financial Studies*, 34(11):5149–5187.
- Friedkin, N. E. and Johnsen, E. D. (1999). Social influence networks and opinion chance. *Advances in Group Processes*, 16:1–29.
- Fuster, A., Kaplan, G., and Zafar, B. (2018). Wht would you do with \$500? Spending responses to gains, losses, news and loans. *NBER working paper*, Review of Economic Studies, R&R.

- Gallipoli, G. and Makridis, C. (2018). Structural Transformation and the Rise of Information Technology. *Journal of Monetary Economics*, 97:91–110.
- Gallipoli, G. and Makridis, C. A. (2022). Sectoral Digital Intensity and GDP Growth After a Large Employment Shock: A Simple Extrapolation Exercise. *Canadian Journal of Economics*, 55(S1):446–479.
- Gillitzer, C. and Prasad, N. (2018). The effect of consumer sentiment on consumption: Cross-sectional evidence from elections. *American Economic Journal: Macroeconomics*, 10(4):234–269.
- Giuliano, P. and Spilimbergo, A. (2014). Growing up in a Recession. *Review of Economic Studies*, 81(2):787–817.
- Goldsmith-Pinkham, P. and Imbens, G. W. (2013). Social Networks and the Identification of Peer Effects. *Journal of Business & Economic Statistics*, 31(3):253–264.
- Golub, B. and Jackson, M. O. (2010). Naive learning in social networks and the wisdom of crowds. *American Economic Journal: Microeconomics*, 2(1):112–49.
- Gourinchas, P.-O. and Parker, J. A. (2002). Consumption over the life cycle. *Econometrica*, 70(1):47–89.
- Guerrieri, V., Lorenzoni, G., Straub, L., and Werning, I. (2020). Macroeconomic Implications of COVID-19: Can Negative Supply Shocks Cause Demand Shortages? *NBER working paper*.
- Heathcote, J., Perri, F., and Violante, G. L. (2010). Unequal we stand: An empirical analysis of economic inequality in the United States, 1967-2006. *Review of Economic Dynamics*, 13:15–51.
- Heathcote, J., Storesletten, K., and Violante, G. L. (2014). Consumption and labor supply with partial insurance: An analytical framework. *American Economic Review*, 104(7):1–52.
- Hirshleifer, D., Peng, L., and Wang, Q. (2023). News diffusion in social networks and stock market reactions. Technical report, National Bureau of Economic Research.
- Huang, A., Makridis, C. A., Baker, M., Medeiros, M., and Guo, Z. (2020). Understanding the Impact

- of COVID-19 Intervention Policies on the Hospitality Labor Market. *International Journal of Hospitality Management*, 91.
- Jappelli, T. and Pistaferri, L. (2010). The consumption response to income changes. *Annual Review of Economics*, 2:479–506.
- Johnson, D. S., Parker, J. A., and Souleles, N. S. (2006). Household expenditure and the income tax rebates of 2001. *American Economic Review*, 96(5):1589–1610.
- Kaplan, G. and Violante, G. L. (2010). How much consumption insurance beyond self-insurance. *American Economic Journal: Macroeconomics*, 2(4):53–87.
- Kaplan, G. and Violante, G. L. (2014). A model of the consumption response to fiscal stimulus payments. *Econometrica*, 82(4):1199–1239.
- Krueger, D., Uhlig, H., and Xie, T. (2022). Macroeconomic dynamics and reallocation in an epidemic: evaluating the “Swedish solution”. *Economic Policy*, 37(110):341–398.
- Kuchler, T., Piazzesi, M., and Stroebel, J. (2023). Housing Market Expectations. *Handbook of Economic Expectations*.
- Kuchler, T. and Zafar, B. (2019). Personal experiences and expectations about aggregate outcomes. *Journal of Finance*, 74(5):2491–2542.
- Makridis, C. A. (2022). The Social Transmission of Economic Sentiment on Consumption. *European Economic Review*, 148(104232).
- Makridis, C. A. and Hartley, J. (2020). The cost of COVID-19: A rough estimate of the 2020 GDP impact. *Mercatus Center, Policy Brief Special Edition*.
- Makridis, C. A. and McGuire, E. (2020). Refined by Fire: The Great Depression and Entrepreneurship. *Working paper*.
- Malmendier, U. and Nagel, S. (2011). Depression babies: Do macroeconomic experiences affect risk taking? *Quarterly Journal of Economics*, 126(1):373–416.

- Malmendier, U. and Nagel, S. (2016). Learning from inflation experiences. *Quarterly Journal of Economics*, 131(1):53–87.
- Malmendier, U., Pouzo, D., and Vanasco, V. (2018). Investor experiences and financial market dynamics. *NBER Working Paper 24697*.
- Malmendier, U. and Shen, L. S. (2021). Scarred consumption. *American Economic Journal: Macroeconomics*, forthcoming.
- Manski, C. F. (1993). Identification of endogenous social effects: The reflection problem. *The review of economic studies*, 60(3):531–542.
- Manski, C. F. (2000). Economic analysis of social interactions. *Journal of economic perspectives*, 14(3):115–136.
- Piazzesi, M. and Schneider, M. (2009). Momentum traders in the housing market: Survey evidence and a search model. *American Economic Review*, 99(2):406–411.
- Pistaferri, L. (2001). Superior information, income shocks, and the permanent income hypothesis. *Review of Economics and Statistics*, 83(3):465–476.
- Ritter, Z. (2020). Americans Use Social Media for COVID-19 Info, Connection. *Gallup*.
- Shiller, R. J. and Pound, J. (1989). Survey evidence on diffusion of interest and information among investors. *Journal of Economic Behavior & Organization*, 12(1):47–66.
- Smith, A. and Anderson, M. (2018). Social media use in 2018. *Pew Center*.
- Souleles, N. S. (1999). The response of household consumption to income tax refunds. *American Economic Review*, 89(4):947–958.
- Ugander, J., Karrer, B., Backstrom, L., and Marlow, C. (2011). The anatomy of the facebook social graph. *arXiv preprint arXiv:1111.4503*.
- vom Lehn, C. and Winberry, T. (2020). The investment network, sectoral comovement, and the changing U.S. business cycle. *Quarterly Journal of Economics, R&R*.

- Westerman, D., Spence, P. R., and Van Der Heide, B. (2014). Social media as information source: Recency of updates and credibility of information. *Journal of Computer-Mediated Communication*, 19(2):171–183.
- Zeldes, S. P. (1989). Consumption and liquidity constraints: An empirical investigation. *Journal of Political Economy*, 97(2):305–346.

A Online Appendix

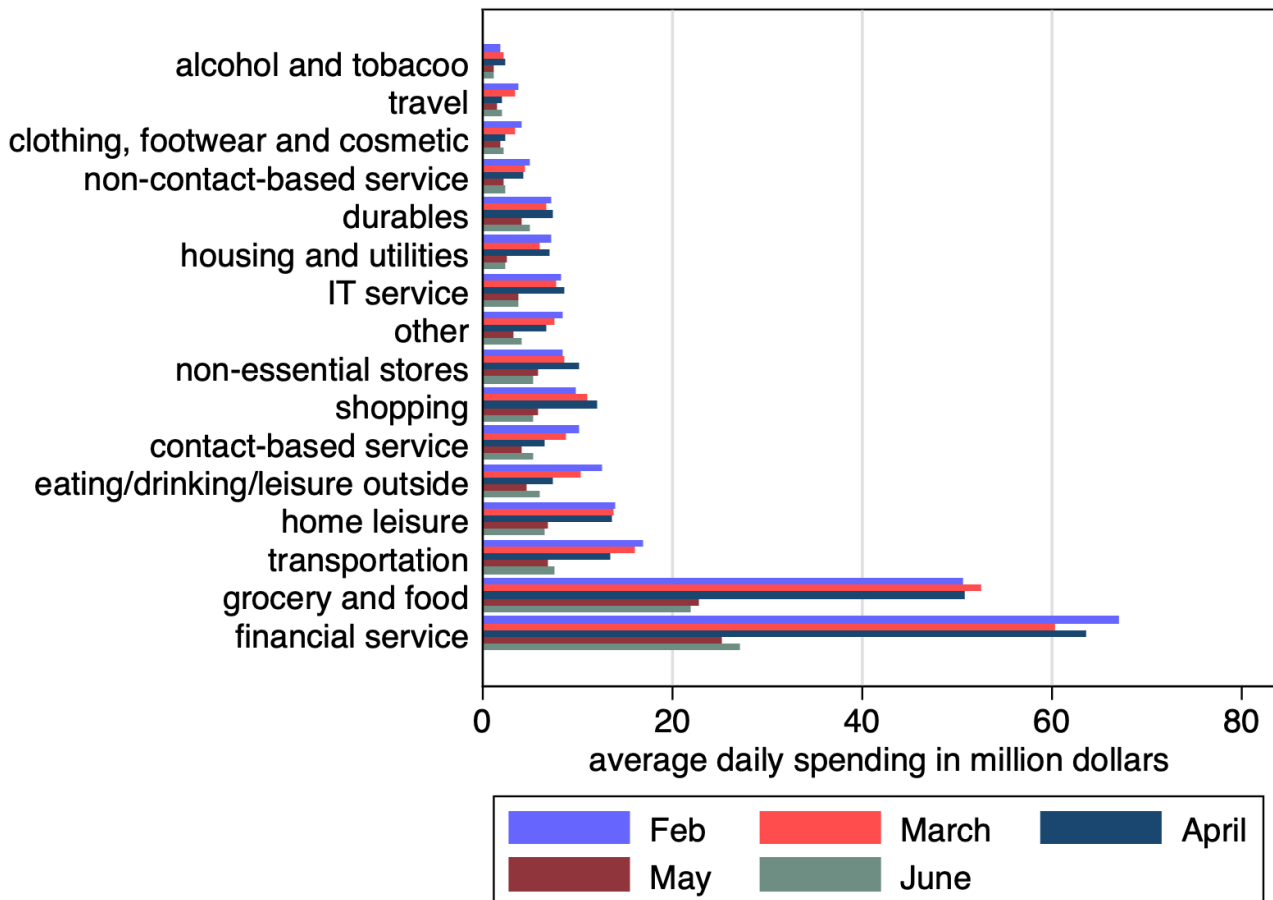
A.1 Validation of the consumption spending data

Figure A.1 plots the average daily spending of each month since February 2020 by consumption category. The bulk of the consumption is accounted for by goods and services that are generally most exposed to the pandemic, including eating and drinking, leisure outside of the home, contact-based services, travel and transportation, and clothing, footwear, and cosmetics. However, some goods and services, such as financial services, grocery shopping, and home leisure, have actually increased in March, relative to the two months prior. One important difference in the data, however, is that grocery shopping and other necessary purchases account for a large share in total spending, reflecting the fact that the composition of consumers in the sample is lower income and younger than a more nationally representative sample.

While the data contains these three important advantages over the traditional sources, we nonetheless are concerned about whether the data is nationally representative enough to map elasticities identified in the micro-data to the aggregate economy. We explore several validation exercises. First, Figure A.2 plots monthly total spending in contact and non-contact sectors based on our transaction records and the advanced retail sales provided by the Census Bureau. For each sector, we combine sub-category series to make the retail sales data approximately comparable with that constructed from the transactions. Specifically, the contact-based consumption for retail sales is approximated by the sum of “drinking and eating places” (RSFSDP) and “health and personal car” (RSHPCS). The non-contact consumption is approximated as the total of “grocery store” (RSGCS) and “food and beverage stores” (RSDBS).

As shown in the Figure A.2, in both sectors, our separately constructed time series track with

Figure A.1: Descriptive Statistics on Consumption Expenditures, by Category



Notes.—Source: Facteus. Average daily consumption by category. Each bar plots the average spending per day in the specific category within each month. See the Appendix for the examples of each consumption category.

each other reasonably well, although they are not apples to apple comparisons—the correlation is 0.55 in non-contact consumption and 0.26 in contact consumption over the four-year period that overlaps.²³ Despite the lower correlation in contact consumption, importantly, both series mark a dramatic drop in spending in March 2020 and a similar recovery since late April. In its trough, the retail sales and food service decreased by around 16.4% from the same month last year. Given our empirical analysis primarily rely upon the subsample of the year 2020, we are additionally assured

²³Some of the differences between the two series may emerge because the sample selects lower-income individuals and does not have complete coverage throughout the country. These low income and younger groups are widely known in the literature to have a high Engel index, i.e. a large share of spending on necessities such as grocery/food. That means the composition of the spending recorded in the transaction is geared toward basic items. Moreover, both low-income and young people tend to have a high marginal propensity to consume (MPC) due to under insurance. This will undoubtedly induce more volatility in consumption spending across different periods.

about the representativeness of our results.

Figure A.2: Benchmarking Consumption Expenditures with Retail Sales Over Time



Notes.—Source: retail sales from the Census Bureau and transaction data from Facteus from June 2017 to June 2020. The upper and bottom figures plot the contact and non-contact consumption, respectively. See the appendix for the classification of card transactions. Both retail sales and transactions are without seasonal adjustment and deflated by the PCE price index. Contact-based consumption for retail sales is approximated by the sum of “drinking and eating place” (RSFSDP) and “health and personal care” (RSHPCS). The non-contact consumption is approximated as the total of “grocery stores” (RSGCS) and “food and beverage stores” (RSDBS). The correlation coefficient of the two series is 0.26 and 0.55 on the top and bottom, respectively.

A.2 Data Description: Consumption Classification

Grocery and food. 1. grocery stores and supermarkets; 2. convenience stores; 3. drug stores and pharmacies; 4. miscellaneous retail stores; 5. meat provisions; 6. bakery, etc.

Transportation. 1. bus lines; 2. railway stations 3. car rentals; 4. toll and bridge fees, etc.

Home leisure. 1. TV cable fees; 2. digital goods, i.e. games, etc.

Housing and utilities. 1. housing rent payment; 2. home utilities, etc.

Shopping. 1. department stores; 2. discount stores; 3. variety stores; 4. general merchandise; 5. wholesale clubs, etc.

Eating, drinking, and leisure outside the home. 1. restaurants; 2. bars/taverns/clubs; 3. different kinds of parks; 4. outdoor sport and sports events; 5. orchestra and theaters, etc.

Information technology services. 1. computer network; 2. telegraph; 3. telecommunication, etc.

Contact-based services. 1. barber and beauty shops; 2. child care; 3. home cleaning; 4. repair stores; 5. veterinary services; 6. home furnishing; 7. laundry; 8. auto repair, etc.

Durables. 1. vehicles/motorcycle /auto parts; 2. furniture; 3. home appliances; 4. electronics and equipment; 5. home supplies; 6. music instruments, etc.

Non-contact-based services. 1. accounting/auditing; 2. business services; 3. programming; 4. consultations; 5. horticultural/ landscaping, etc.

Clothing, footwear, and cosmetics. 1. clothing stores of different kinds; 2. cosmetic stores; 3. footwear and shoe stores, etc.

Alcohol and tobacco. 1. package stores selling wine, beer and other liquor; 2. cigar and tobacco stores, etc.

Travel. 1. airlines; 2. lodging and hotels; 3. duty-free stores; 4. airports; 5. travel agencies, etc.

Financial services. 1. insurance; 2. money orders; 3. wire transfers, etc.

Other. 1. public organizations; 2. government fees; 3. educations; 4. medical spending such as a dental clinic, etc.

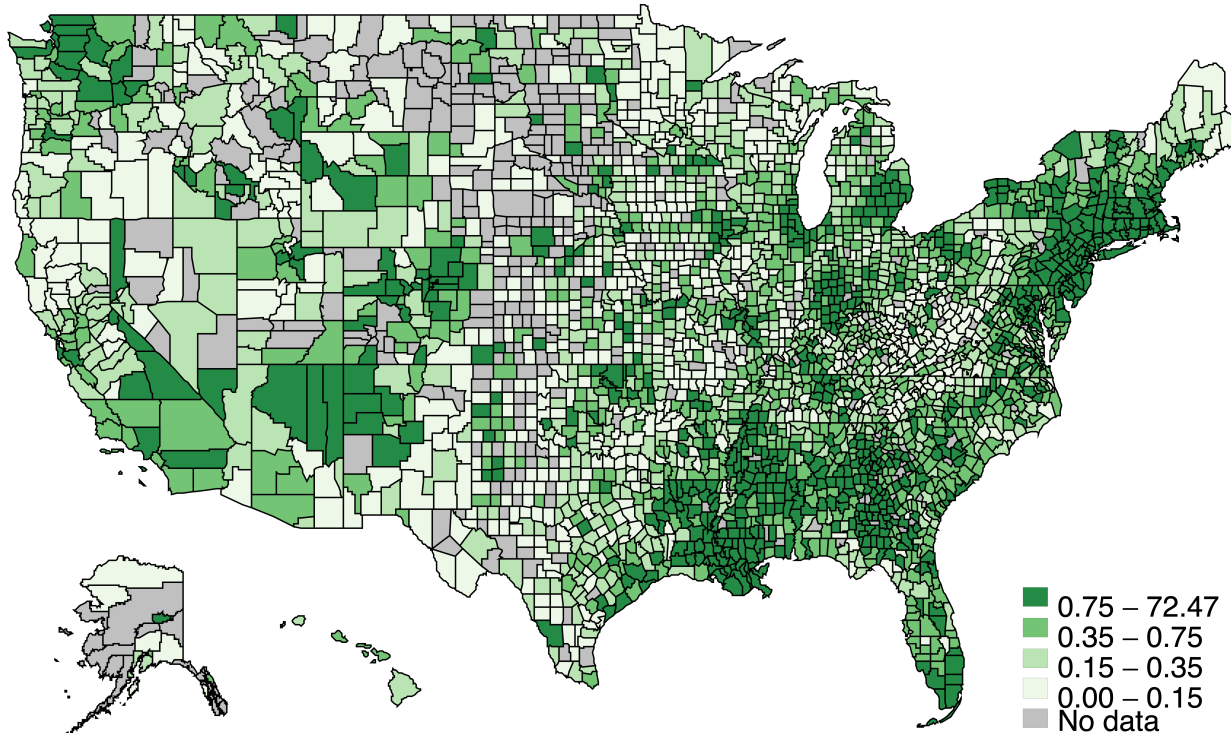
In our model with two broad sectors of consumption, contact-based consumption includes transportation, shopping, eating/drinking/leisure outside the home, contact-based services, durables, clothing/footwear, and cosmetics travel. Non-contact consumption includes grocery and food, home leisure, housing and utilities, information technology services, non-contact-based services, alcohol and tobacco, and financial services.

A.3 Data Description: Social Connectedness Index

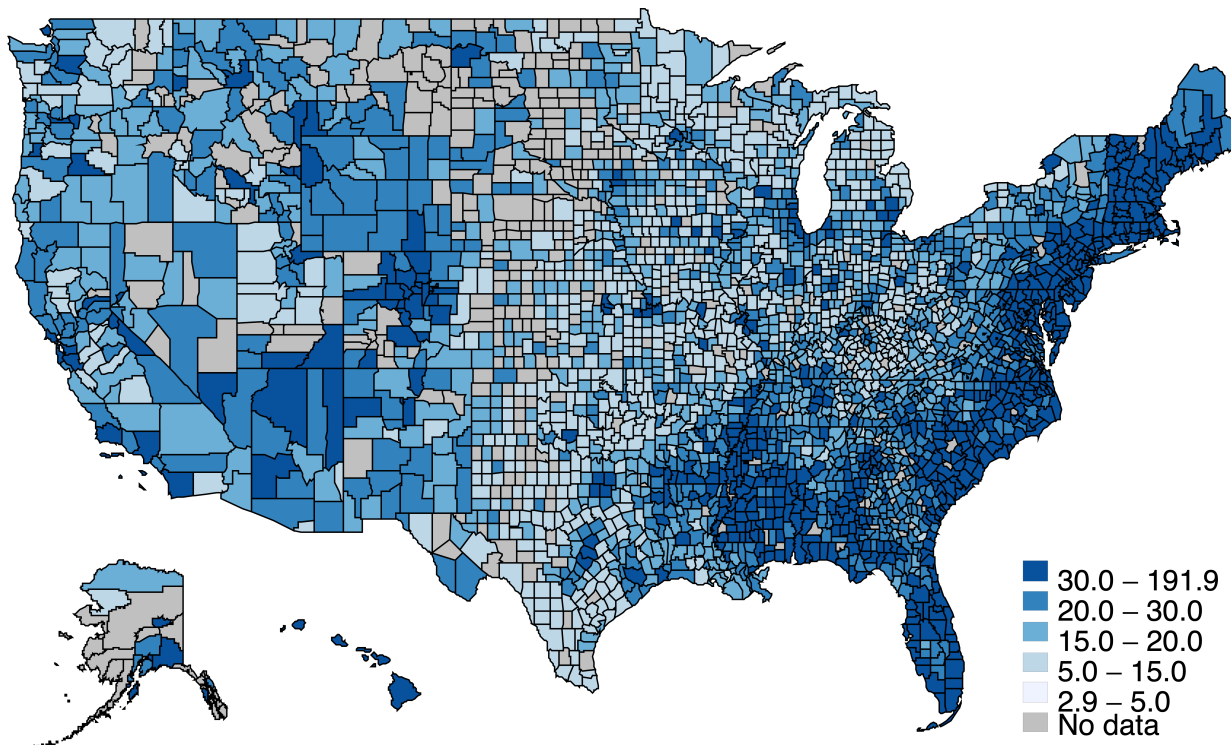
Figures A.3 and A.4 characterize the spatial distribution of not only infections and deaths, but also SCI-weighted cases and deaths based on exposure to connected counties as of April 1, 2020. While the actual number of infections or deaths in a county c are correlated with their SCI-weighted versions, they display important differences. In particular, the correlation is only 0.40 between infections / deaths and their SCI counterparts. Moreover, the correlation is roughly half as large when comparing SCI-weighted infections and deaths or infections and SCI-weighted deaths.

Figure A.3: Actual and Socially-connected COVID-19 Case Infections

Nb of cases per thousand (Apr 1st 2020)



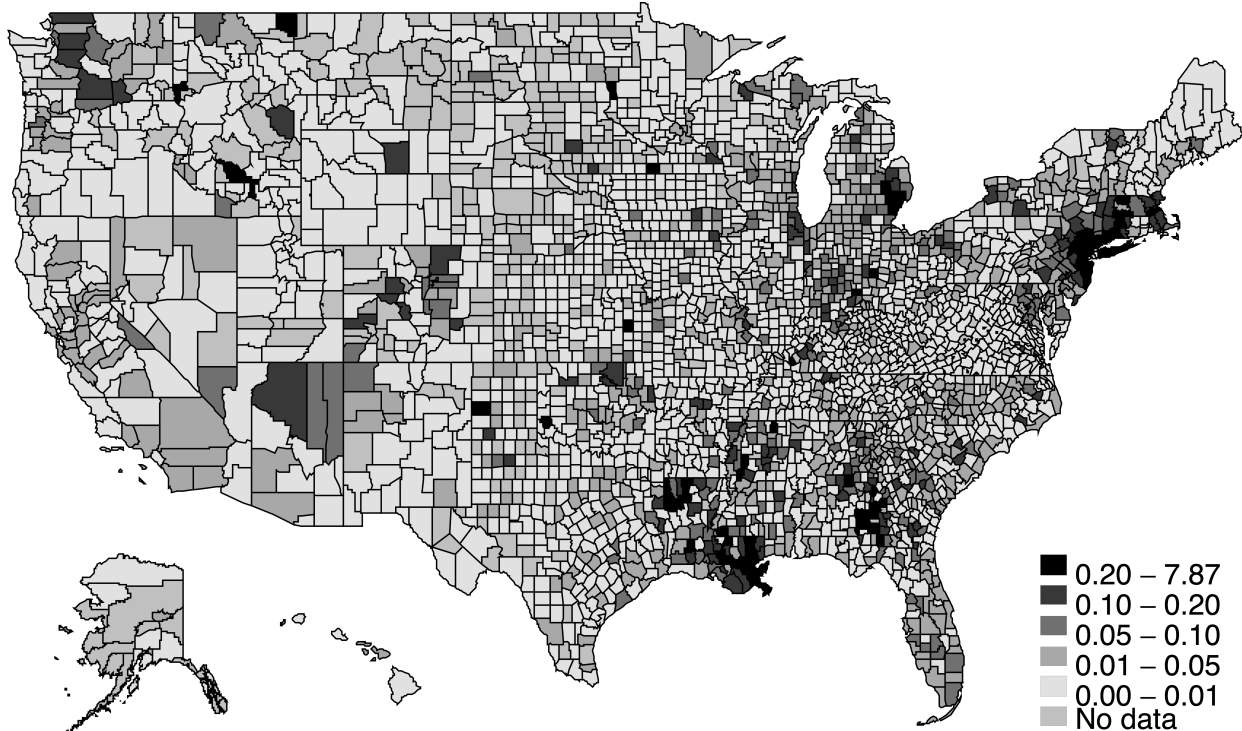
Nb of cases per thousand on Facebook (Apr 1st 2020)



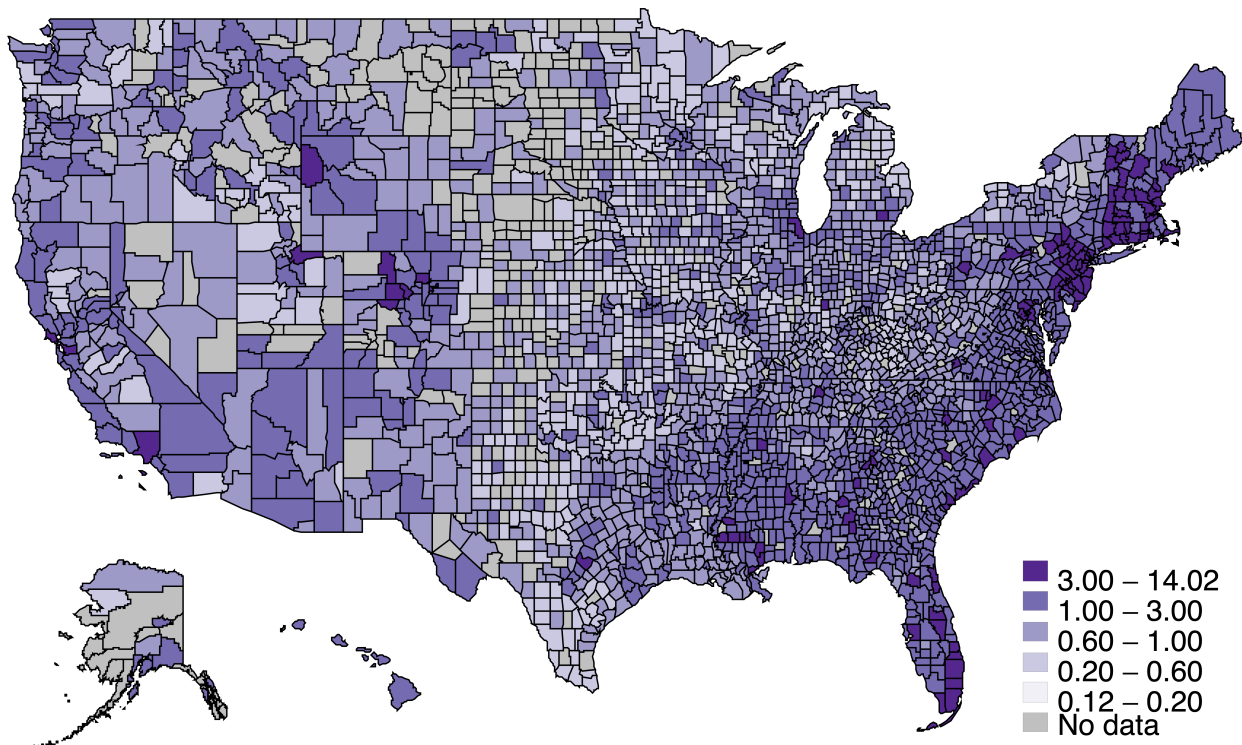
Notes.—Source: Facebook 2019 Social Connectedness Index (SCI). Panel A plots the number of COVID-19 infections per 1,000 individuals within each county as of April 1st, 2020. Panel B plots the SCI-weighted number of infections per 1,000 individuals, obtained by taking the population-weighted average across the product of infections in county c' and the SCI between county c and c' .

Figure A.4: Actual and Socially-connected COVID-19 Deaths

Nb of deaths per thousand (Apr 1st 2020)

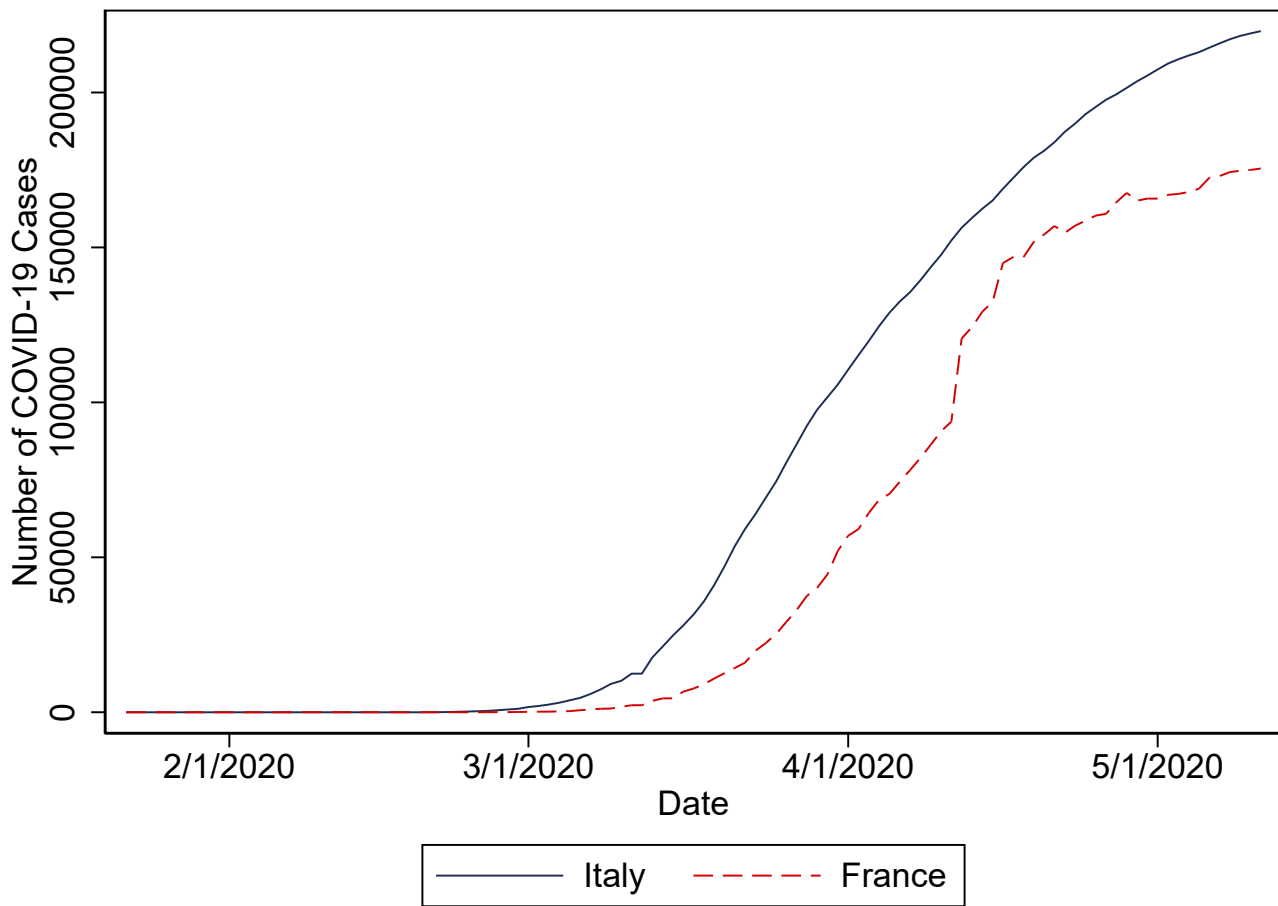


Nb of deaths per thousand on Facebook (Apr 1st 2020)



Notes.—Source: Facebook 2019 Social Connectedness Index (SCI). Panel A plots the number of COVID-19 deaths per 1,000 individuals within each county as of April 1st, 2020. Panel B plots the SCI-weighted number of deaths per 1,000 individuals, obtained by taking the population-weighted average across the product of deaths in county c' and the SCI between county c and c' .

Figure A.5: Time Series Patterns in COVID-19 Infections: Italy and France

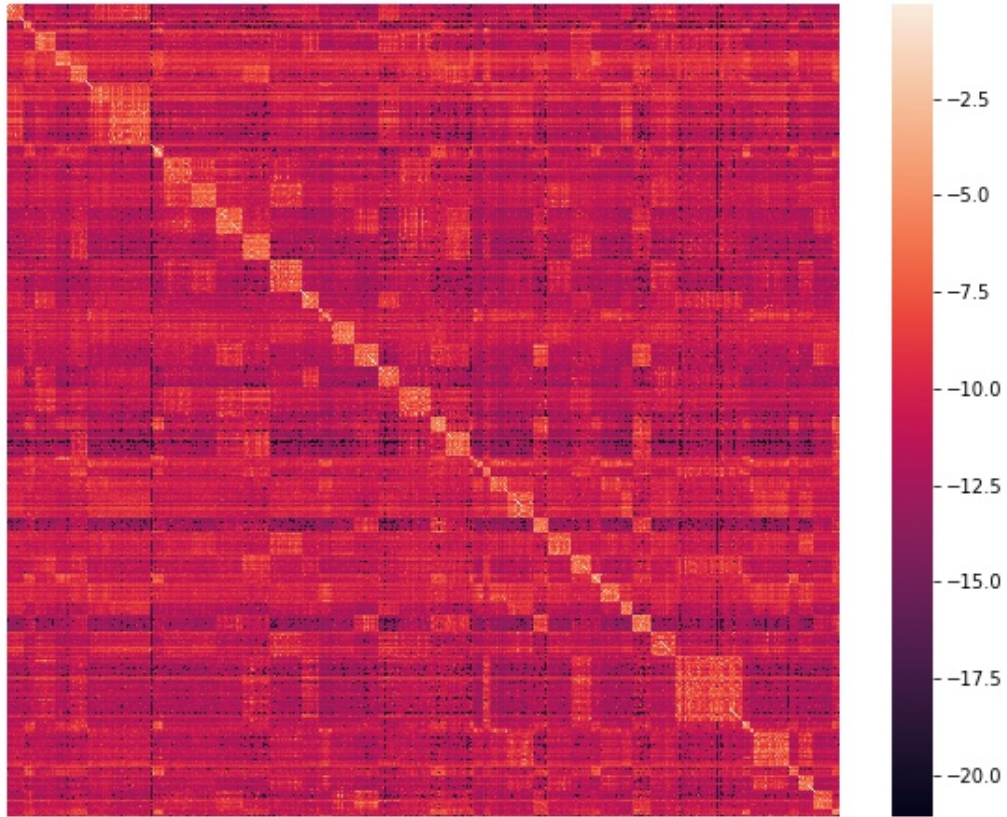


Notes.—Source: Johns Hopkins. The figure plots the number of COVID-19 infections for Italy and France over time.

Figure A.6 presents the heat map corresponding to the listening matrix using 2019 SCI data. It demonstrates the significant variability across counties.

Figure A.7 plots the distribution of degrees from the SCI in the years 2016 and 2019, respectively. The distribution is right-skewed with a long tail. This indicates a small fraction of nodes has a disproportionately strong influence within the network. By construction, the average degree in the network is 1. The observed standard deviation, a measure of the dispersion of influences, is 0.27 in 2016 and 0.29 in 2019, respectively. This suggests that social network connections have grown more dispersed over time. All symmetric matrices have the property that all nodes are of degree 1

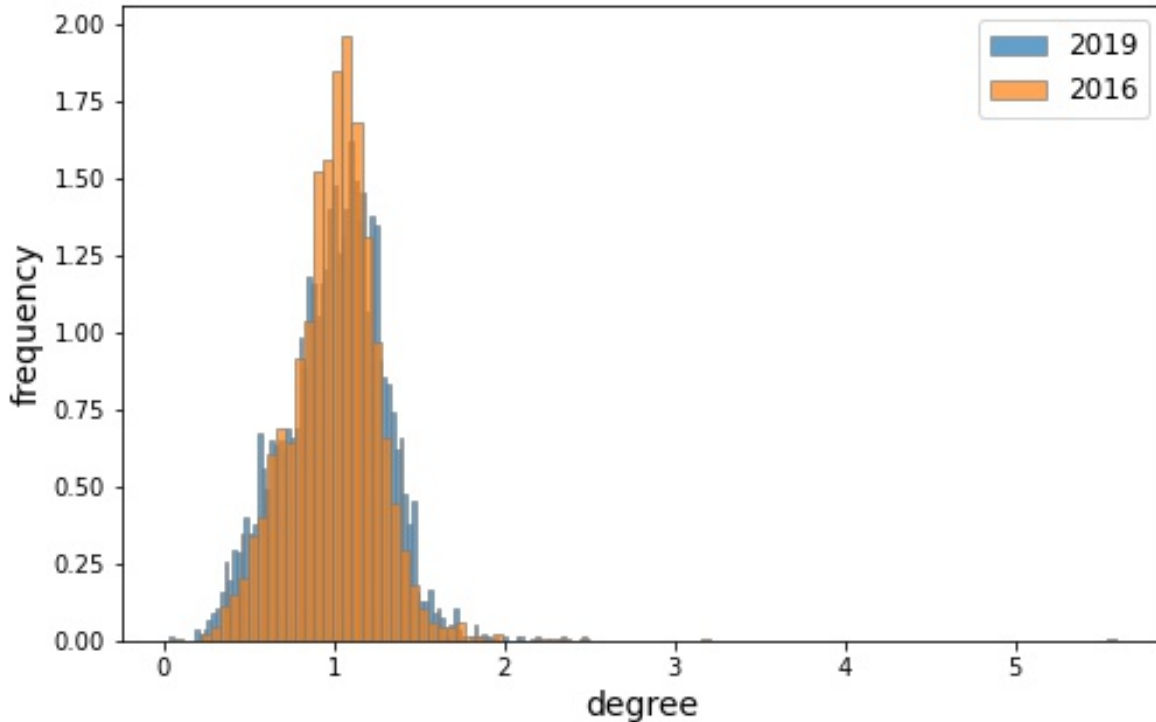
Figure A.6: Listening Matrix Across Counties



Notes.—Source: Facebook 2019 Social Connectedness Index (SCI). The heatmap plots the logged listening matrix of 3141 U.S. counties according to SCI data of 2019. The matrix W is defined as in Equation ???. The i -th row and j -th column entry of the W , $w_{i,j}$, represents the social influence the j -th node has on i -th node in the network.

thus zero-dispersion represents. In contrast, higher dispersion of the degrees implies the nodes have more asymmetric influences on others across the network. A more disperse distribution in 2019 compared to 2016 will lead to a higher degree of amplification of local shocks to the whole network, albeit small, as we will see in the next sections. These differences across the network imply that the aggregate fluctuations in consumption will depend on where the initial shocks take place.

Figure A.7: Distribution of the Degree of Direct Influences in the Network

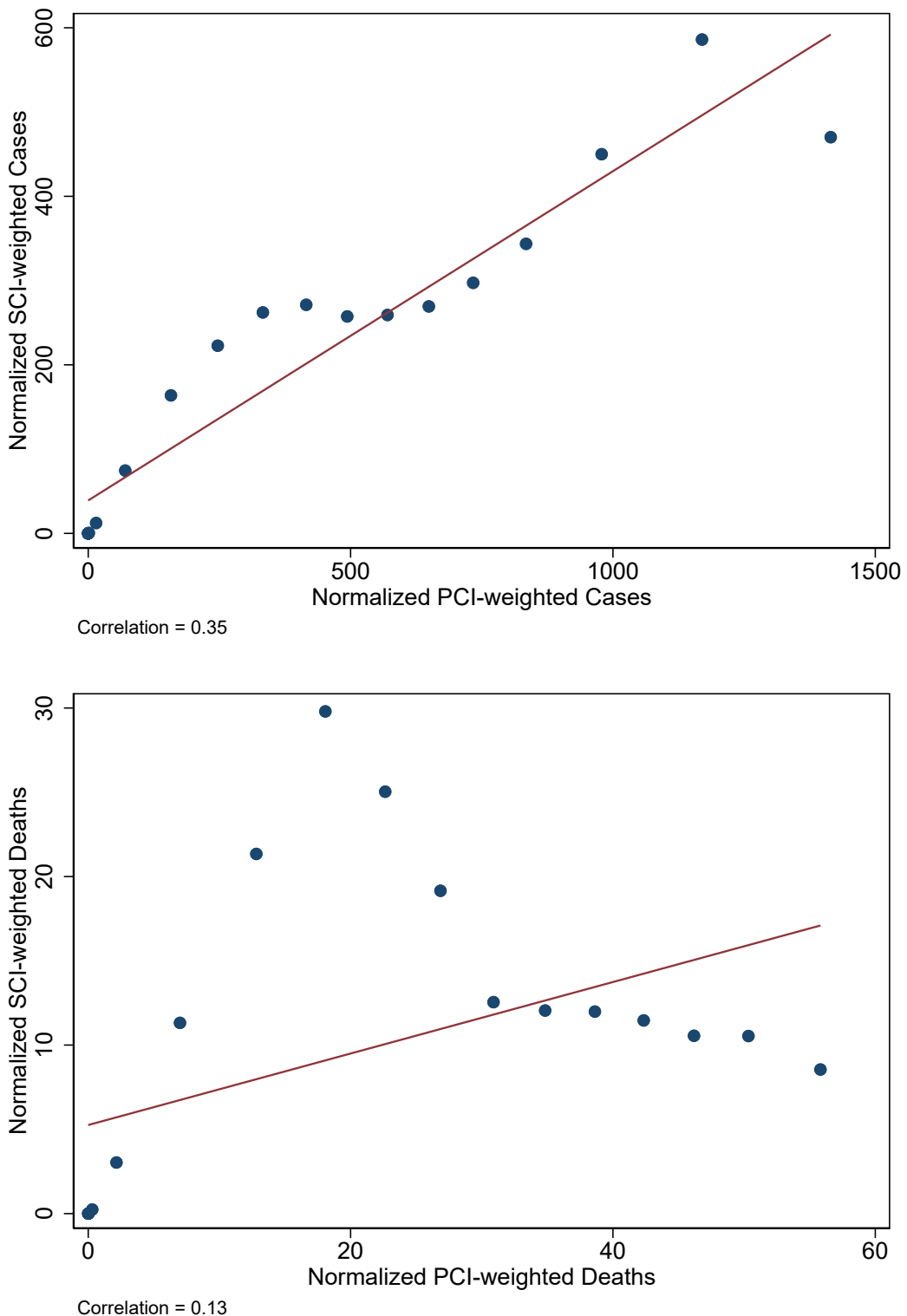


Notes.—Source: Facebook Social Connectedness Index (SCI) for 2016 and 2019. The histogram plots the distribution of degrees of 3141 counties according to SCI’s 2016 and 2019 extracts, respectively. The degree is defined as in Equation ??.

A.4 Supplement to the Empirical Results

We now explore several robustness exercises to our main empirical results that show how increases in the number of SCI-weighted cases are associated with declines in consumption. One of our concerns is that social connectivity is simply a proxy for physical proximity. We examine this concern by obtaining the distance from each county to every other county, just as in our SCI data, and use it to construct a similar index for coronavirus cases, which we call the physical connectedness index (PCI). Figure A.8 documents these results, showing that there is only a correlation of 0.35 (0.13) between the SCI and PCI -weighted number of coronavirus cases (deaths). This suggests that social connectivity is not simply capturing differences in physical distance.

Figure A.8: Social and Physical Connectedness -Weighted Coronavirus Cases & Deaths



Notes.—Sources: Facebook Social Connectedness Index and the NBER Physical Distance data. The figure documents the number of coronavirus cases and deaths constructed using the physical and social connectedness indices normalized to the total distance and number of friendship ties.

We subsequently investigate the role of physical distance in greater detail by replicating the main results under different specifications with physical distance as a control. Table A.1 documents these results. We present the simple specification in columns 1 and 5: a 10% rise in SCI-weighted cases and deaths is associated with a 0.5% and 0.16% decline in consumption expenditures. After we add PCI-weighted cases and deaths, our main results are not significantly altered: our coefficient on logged SCI-weighted cases is statistically indistinguishable and the coefficient on logged SCI-weighted deaths is even larger (columns 2 and 6). Columns 3 and 7 subsequently add time-varying state policy controls, which only reduces the magnitude of our coefficients marginally. Finally, columns 4 and 8 add two-week lagged values of logged coronavirus cases and deaths. Although the coefficients decline in magnitude, the main results remain statistically and economically significant. We also note that PCI-weighted cases are not associated with consumption, but PCI-weighted deaths is strongly negatively correlated with consumption.

In summary, these results show that our SCI-weighted coronavirus cases and deaths index is not simply capturing variation in physical distance. Moreover, even when we control explicitly for a comparable measure of PCI-weighted cases and deaths, our results remain. These exercises are on top of the baseline specification, which excludes counties in the same state (otherwise closely connected geographies).

Since our consumption data is based on a sample of debit-card users that is disproportionately represented by young and low-income people, it is also worth checking if the empirical results are robust to an alternative measure of consumer spending from a separate data source. We utilize the county-level consumer spending of 1481 counties across the United States based on both debit and credit card transaction data provided by Affinity, a commercial provider.²⁴ Table A.2 reports the results of the same regression as the baseline, except for replacing the dependent variable with the

²⁴Chetty et al. (2020) shows that the aggregate series of the transaction data tracks the national retail sales (excluding auto and gas) from the Monthly Retail Trade Survey remarkably well.

Table A.1: Examining the Role of Physical Distance for Predicting Consumption Responses

Dep. var. =	log(Consumption Expenditures)							
	(1)	(2)	(3)	(4)	(5)	(6)	(7)	(8)
log(SCI-weighted Cases)	-.051*** [.004]	-.050*** [.006]	-.042*** [.007]	-.017** [.008]				
log(SCI-weighted Deaths)					-.016** [.007]	-.050*** [.006]	-.046*** [.006]	-.023*** [.009]
log(PCI-weighted Cases)	.007 [.018]	.006 [.018]	.026 [.017]					
log(PCI-weighted Deaths)						-.175*** [.016]	-.175*** [.015]	-.157*** [.015]
log(County Cases), 14 day Lag				-.018*** [.004]				-.022*** [.004]
log(County Deaths), 14 day Lag				.008 [.006]				.011** [.005]
R-squared	.99	.99	.99	.99	.99	.99	.99	.99
Sample Size	351644	351644	351644	351644	351644	351644	351644	351644
County FE	Yes	Yes	Yes	Yes	Yes	Yes	Yes	Yes
Time FE	Yes	Yes	Yes	Yes	Yes	Yes	Yes	Yes
State Policies	No	No	Yes	Yes	No	No	Yes	Yes

Notes.—Sources: Facebook Social Connectedness Index (SCI) for 2019, Facteus. The table reports the coefficients associated with regressions of logged consumption spending on logged SCI and PCI -weighted infections (excluding county c 's friendship ties with itself) and logged county infections and deaths, conditional on county and time fixed effects. Consumption is deflated by the national personal consumption expenditure index. Our SCI-weighted cases and death index is constructed as follows: $COVID_{c,t}^{SCI} = \sum_{c'} (COVID_{c',t} \times SCI_{c,c'})$ where $COVID_{ct}^{SCI}$ denotes the logged SCI-weighted number of cases or deaths in connected counties, $COVID_{c',t}$ denotes the logged number of cases or deaths in county c' , and $SCI_{c,c'}$ denotes our measure of the SCI. We normalize the scaled number of friendship ties in a county to its total number of friendship ties, thereby exploiting the relative exposure to other locations. The physical connectedness index (PCI) is constructed similar using miles between counties, rather than friendship ties. Our variables that are denoted “other states” construct the SCI excluding counties within the same state to control for physical proximity. Standard errors are clustered at the county-level and observations are weighted by county population. The sample period is between March 1st to June 30th, 2020.

growth rate relative to January 2020 of each day. The negative and significant coefficients associated with the SIC weighted cases and deaths remain negative and significant.

Table A.2: Alternative Data Source of Consumption Spending

Dep. var. =	log(Consumption Expenditures) Growth							
	(1)	(2)	(3)	(4)	(5)	(6)	(7)	(8)
Has SAHO			-.011*** [.003]	.015** [.007]			-.010*** [.003]	-.008** [.003]
log(SCI-weighted Cases)	-.028*** [.004]	-.018*** [.005]	-.029*** [.004]	-.025*** [.004]				
× SAHO					-.008*** [.002]			
log(SCI-weighted Deaths)						-.023*** [.003]	-.024*** [.004]	-.042*** [.005]
× SAHO								-.004* [.002]
log(County Cases)	.000 [.002]	.002 [.002]	.002 [.002]			-.003* [.001]	-.001 [.001]	-.001 [.001]
log(County Deaths)	-.007*** [.003]	-.007*** [.001]	-.007*** [.001]			.003 [.002]	.001 [.002]	.001 [.002]
R-squared	.84	.84	.75	.75	.73	.73	.75	.75
Sample Size	175857	175857	175857	175857	175857	175857	175857	175857
County FE	Yes	Yes	Yes	Yes	Yes	Yes	Yes	Yes
Time FE	Yes	Yes	Yes	Yes	Yes	Yes	Yes	Yes
State Policies	No	No	Yes	Yes	No	No	Yes	Yes
State x Month FE	No	No	Yes	Yes	No	No	Yes	Yes

Notes.—Sources: Facebook Social Connectedness Index (SCI) for 2019, Affinity Solutions. The table reports the coefficients associated with regressions of logged consumption spending growth from January 1st on logged SCI-weighted infections and logged county infections and deaths, conditional on county and time fixed effects. The consumption spending is from the Affinity Solution, including both debit and credit card transactions of consumption spending at the county level.

A.5 Derivations and Proofs of Model Results

Steady state of the Kalman filtering

Under efficient updating using Kalman filtering, the weight $\kappa_{i,t}$ evolves as the following.

$$\kappa_{i,t} = \frac{\Sigma_{i,t-1}}{\Sigma_{i,t-1} + \sigma_\theta^2 + \sigma_\eta^2} \quad (19)$$

$$\Sigma_{i,t} = (1 - \kappa_{i,t})(\Sigma_{i,t-1} + \sigma_\theta^2)$$

where $\Sigma_{i,t-1}$ is i's prior uncertainty regarding ψ_t before updating.

Combining the two equations gives

$$\Sigma_{i,t} = \frac{\sigma_\theta^2 + \sigma_\eta^2}{\Sigma_{i,t-1} + \sigma_\theta^2 + \sigma_\eta^2} (\Sigma_{i,t-1} + \sigma_\theta^2) \quad (20)$$

In steady state, $\Sigma_{i,t} = \Sigma^* \quad \forall t$ and $\kappa_{i,t} = \kappa^* \quad \forall t$. We can solve it as

$$\kappa^* = \frac{\sqrt{(\sigma_\theta^2 + \sigma_\eta^2)\sigma_\theta^2}}{\sqrt{(\sigma_\theta^2 + \sigma_\eta^2)\sigma_\theta^2} + \sigma_\theta^2 + \sigma_\eta^2} \quad (21)$$

Evolution of the average belief

We define the average belief of the society at time t by $\tilde{\psi}_t^{av}$ as following, where H is a $1 \times N$ vector and N is the number of agents in the economy.

$$\tilde{\psi}_t^{av} = \frac{1}{N} H \tilde{\psi}_t \quad (22)$$

Using the law of motion of the social belief from Equation 6, we can write v -step-ahead average belief $\tilde{\psi}_{t+v}^{av}$ as a function of realized signals between t and $t+v$ as the following.

$$\tilde{\psi}_{t+v}^{av} = \prod_{h=1}^v M_{t+h} \tilde{\psi}_t^{av} + \frac{1}{N} H \sum_{s=0}^v \prod_{h=1}^s M_{t+h} (1 - \lambda) \kappa_{t+s} s_{t+s} \quad (23)$$

Under constant-gain learning

Under constant-gain learning, we can drop the time script t from κ_t and further assume it to be a constant k across individuals, then κ_t becomes a constant diagonal matrix.

$$\kappa_t = kI \quad \forall t \quad (24)$$

Then time scripts in κ_t and M_t in the Equation 23 all drop.

$$\tilde{\psi}_{t+v}^{av} = M^v \tilde{\psi}_t^{av} + \frac{1}{N} H \sum_{s=0}^v M^s (1 - \lambda) k I s_{t+s} \quad (25)$$

Belief multiplier to exogenous local and aggregate belief shocks

Aggregate effect v periods after a shock to j 's belief

$$\begin{aligned} MP_{t+v|t}^j &= \frac{\overbrace{\delta \tilde{\psi}_{t+v}^{av} / \delta \tilde{\psi}_{j,t} (\lambda \neq 0)}^{\text{social effect+composition effect}}}{\underbrace{\delta \tilde{\psi}_{t+v}^{av} / \delta \tilde{\psi}_{j,t} (\lambda = 0)}_{\text{composition effect}}} \\ &= 1, \quad v = 0 \\ &= \left(\frac{d_j}{1-k} - 1 \right) \lambda + 1 > 1 \quad \text{if } d_j + k > 1, \quad v = 1 \\ &= \frac{\lambda^2}{(1-k)^2} \underbrace{\sum_{s=1}^N d_s w_{s,j}}_{\tilde{d}_j} + \frac{2(1-\lambda)\lambda}{1-k} d_j + (1-\lambda)^2, \quad v = 2 \\ &\dots \end{aligned}$$

where \tilde{d}_j is the friends-weighted influence (degree) of j . $\tilde{d}_j \uparrow$ as $d_j = \sum_{s=1}^N w_{s,j} \uparrow$ $\tilde{d}_j > d_j$ if $d_j > 1$

As a special case, let $\lambda = 1$, then we have

$$MP_{t+v|t}^j = \frac{1}{(1-k)^2} \sum_{s=1}^N d_s w_{s,j} > 1 \quad \text{if } \tilde{d}_j > (1-k)^2$$

The average belief v periods after an exogenous belief shock to all the nodes, the belief multiplier is equal to the sum of individual MP following each node, which is

$$\begin{aligned}
& \sum_{s=1}^N d_s = N \rightarrow \\
& MP_{t+v|t} = \frac{1}{N} \sum_{j=1}^N MP_{t+v|t}^j \\
& = \frac{1}{N} N = 1, \quad v = 0 \\
& = \frac{1}{N} \frac{\sum_{j=1}^N d_j}{1-k} \lambda + (1-\lambda) = \underbrace{\frac{1}{1-k} \lambda}_{\Theta} + (1-\lambda), \quad v = 1 \\
& = \frac{1}{N} \sum_{j=1}^N \tilde{d}_j = \frac{\lambda^2}{(1-k)^2} + \frac{2(1-\lambda)\lambda}{1-k} + (1-\lambda)^2 = \Theta^2, \quad v = 2 \\
& \text{for } \sum_{j=1}^N \tilde{d}_j = \sum_{j=1}^N \sum_{s=1}^N d_s w_{s,j} = \sum_{s=1}^N d_s \sum_{j=1}^N w_{s,j} = N \\
& \dots
\end{aligned} \tag{26}$$

Aggregate belief responses to the aggregate news

The news in our model s_t consists of one aggregate component and an idiosyncratic component which can be stacked up as η_t . The shock to the former, θ_t is permanent, while the latter plays the role of idiosyncratic and serially independent noises by the assumption of the paper.

$$s_t = \xi_t - \xi_{t-1} = \psi_t H' + \eta_t = \psi_{t-1} H' + \theta_t H' + \eta_t \tag{27}$$

Notice the aggregate shock θ_t enters the news permanently, i.e. there is θ_t in s_t, s_{t+1}, \dots . Therefore, the v -step impulse response(IRF) of average belief to θ_t can be summarized by the following scalar.

$$\begin{aligned}
\widetilde{IRF}_{t+v}^{ag} &= \frac{\delta \tilde{\psi}_{t+v}^{av}}{\delta \theta_t} = \frac{1}{N}(1-\lambda)kH \sum_{s=0}^v M^s H' \quad \forall v = 0, 1, \dots \\
&= \frac{1}{N}(1-\lambda)k \sum_{s=0}^v \sum_i^N \sum_j^N m_{i,j}^s
\end{aligned} \tag{28}$$

where $m_{i,j}^s$ is the i,j entry of the matrix M to the power of s . Combining the fact that $\sum_i^N \sum_j^N w_{i,t} = N$, we can show the following.

$$\begin{aligned}
\widetilde{IRF}_{t+v}^{ag} &= \sum_{s=0}^v x^s \\
x^s &= (1-\lambda)k[(1-\lambda)(1-k) + \lambda]^s
\end{aligned} \tag{29}$$

In general, the IRF is a function of λ , k , and the time horizon v . Critically, it does not depend on the network structure W . A trivial case is when $v = 0$, $\widetilde{IRF}_t^{ag} = (1-\lambda)k$, increasing in k and decreasing in λ . This does not depend on W since social communication has not incorporated the newly updated private belief. From $v = 1$ onward, the repeated social communications start propagating these beliefs across society.

The actual v -step-ahead IRF of the ψ_{t+v} to the aggregate shock θ_t is exactly 1. The difference between $\widetilde{IRF}_{t+v}^{ag}$ and 1 characterizes the belief deviation or nowcasting error of the society.

Aggregate belief response to local news

Similarly, we can define the impulse response of average belief to a vector of shocks to the η_t . But the difficulty is that since the response will depend on many details such as the size and the exact locations of each node-specific shock, we cannot derive a close-form formula of IRF for a general $N \times 1$ vector of the shocks.

To proceed, we focus on a special case. If the imagined shock is an equal-sized shock of $\underline{\eta}_t$ (a

scalar) in all the nodes whose influence measured by degree is above a cutoff level \underline{d} . We can more specifically rewrite the shock to η_t as $\underline{\eta}_t Z_t$ where

$$\begin{aligned} Z_t &= [\mathbb{1}(1 \in \Omega), \mathbb{1}(2 \in \Omega), \dots, \mathbb{1}(N \in \Omega)]' \\ \Omega &= \{i \in \{1, 2, \dots, N\} | d_i \geq \underline{d}\} \end{aligned} \tag{30}$$

Combining Equation 27, we can then derive the v step impulse response for this special with respect to $\underline{\eta}_t$ as below.

$$\widetilde{IRF}_{t+v}^{id'} = \frac{\delta \tilde{\psi}_{t+v}^{av}}{\delta \underline{\eta}_t} = \frac{1}{N}(1 - \lambda)kHM^v Z_t \quad \forall v = 0, 1, \dots \tag{31}$$

A special case when $v = 0$, $\widetilde{IRF}_t^{id'} = \frac{1}{N}(1 - \lambda)k \sum_{i=1}^N \mathbb{1}(i \in \Omega)$ and it decreases in both λ and k .

Since all the shocks are idiosyncratic and transitory and the aggregate state ψ_t stays the same, the actual IRF in all horizons is zero. The difference between $\widetilde{IRF}_{t+v}^{id'}$ and zero characterizes social belief deviation from the local shocks.

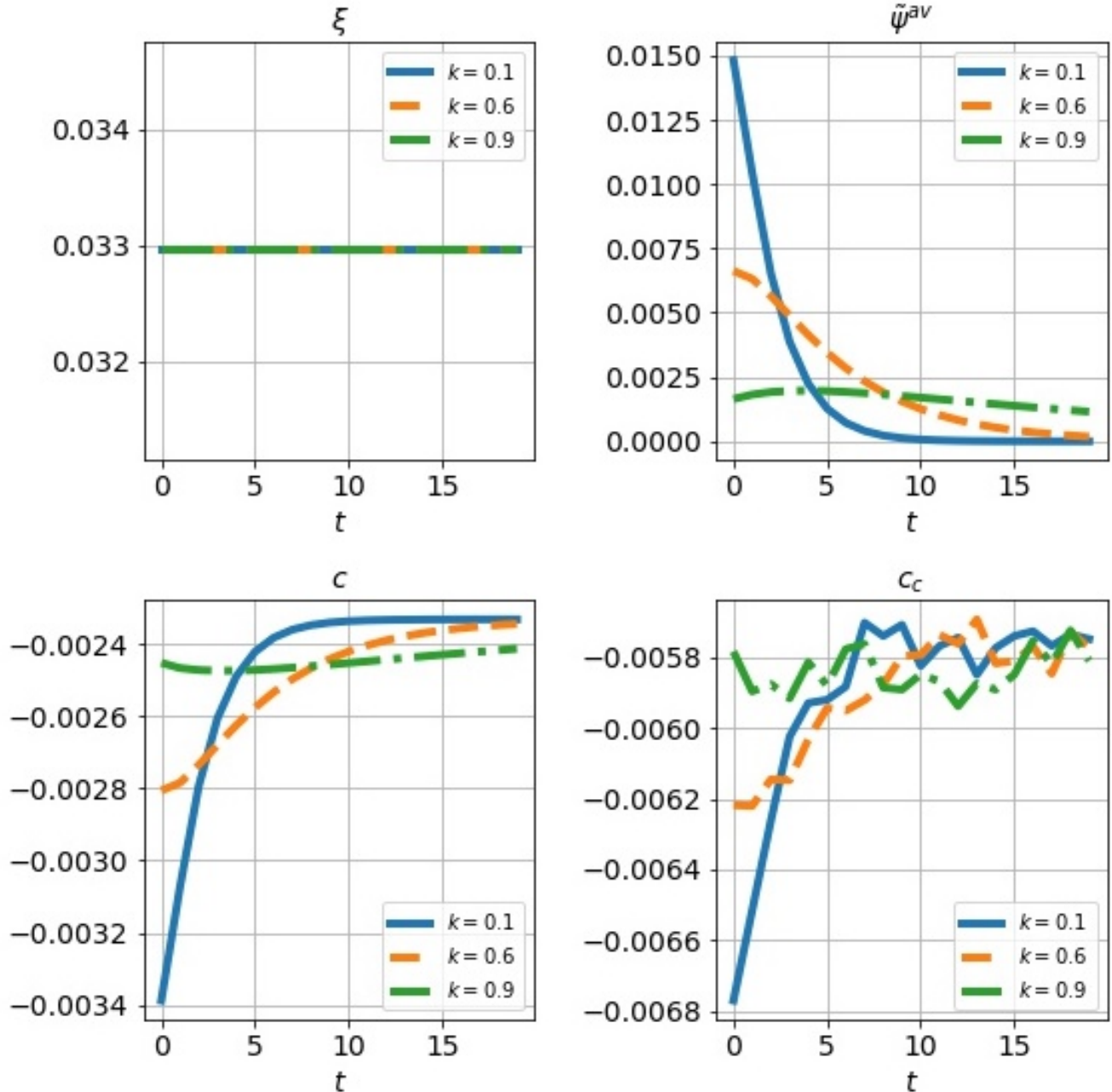
A.6 Other Counterfactual Experiments

A.6.1 Individual Responsiveness to the News

Fixing the degree of social communication at $\lambda = 0.5$, we could explore the consumption responses under different degrees of news responsiveness by individual agents in the model (different k). At the macro level, the effect of higher k and lower λ are similar. Figure A.9 plots the responses. Overreaction to the news at the individual level induces a sharp reaction in aggregate belief but a more rapid reverse to zero. Lower overreaction in contrast slows the spread of the news in general

and smooths both belief reactions and consumption responses.

Figure A.9: Impulse Responses of the Economy to An Infection Shock at Different Degrees of Individual Responsiveness to News



Note: This figure compares the impulse responses of the economy under different degrees of individual responsiveness to the news (k) following a 10% increase in one-third of the agents in the economy whose average degree is greater than 1 at time $t = 0$. The variables are average local infection ξ , average perceived transmission $\tilde{\psi}^{av}$, average total consumption c and average contact-based consumption c_c .

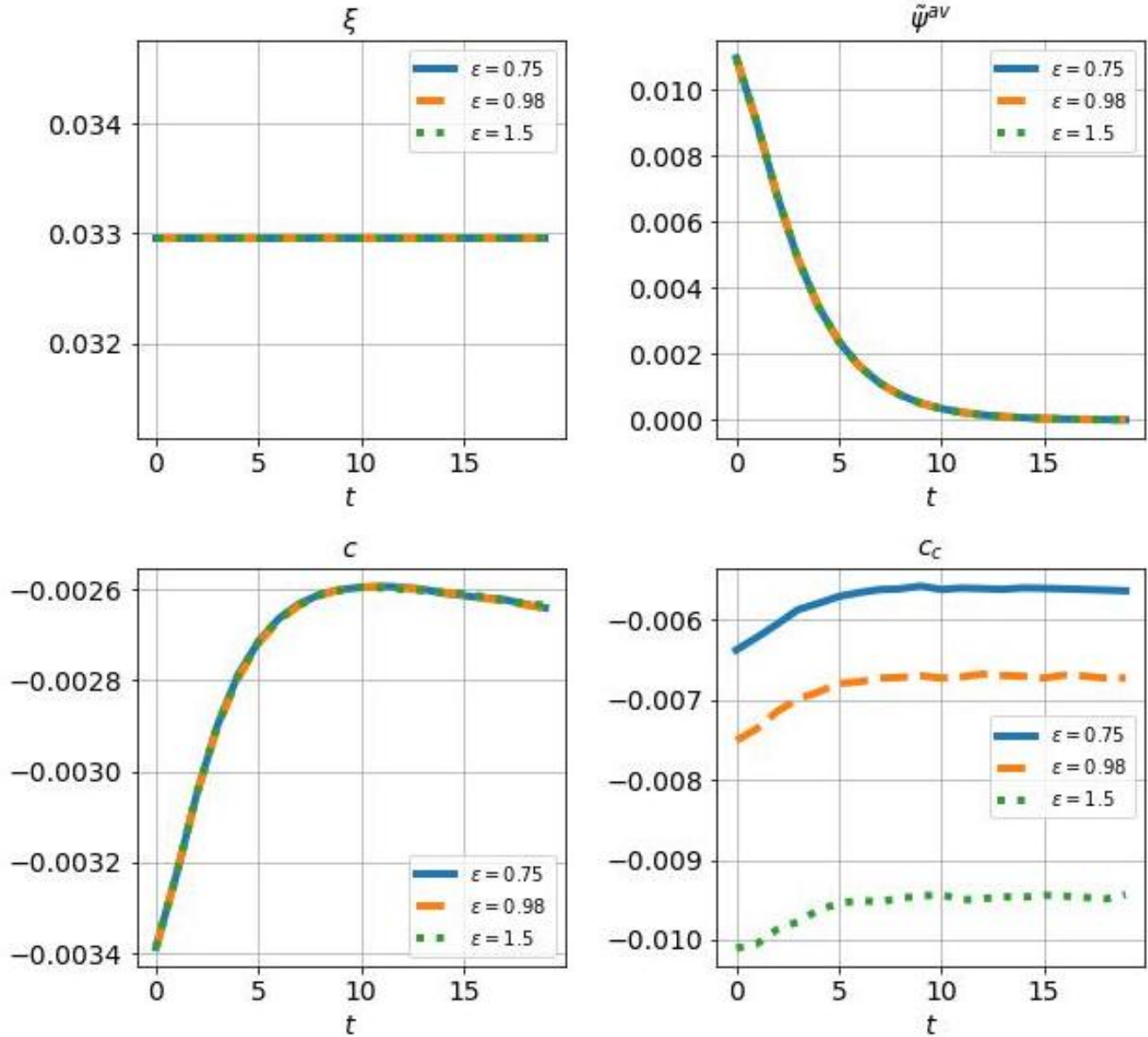
A.6.2 Substitution and Complementarity

In the results thus far, we maintain the assumption that the two sectors of consumption are gross complements. We now compare the impulse responses of following the same shock under a range of values of EOS, 0.75, 0.99 and 1.5. The first is the baseline value we use in the paper. The second represents a case close to unit elasticity. The third is when the two sectors become substitutes. Although the aggregate consumption responses remain the same, the sub-category responses vary substantially depending on whether the two sectors are substitutes or complements for consumer.

Figure A.10 presents the scenario with more substitution, the 0.5% drop in total consumption consists of 1.0% in contact consumption and a 0.2% drop in non-contact consumption. In contrast, the scenario with complementarity implies a different reallocation: 0.8% drop in contact consumption and 0.4% drop in non-contact based consumption.

Such heterogeneity in sectoral reallocation has important implications for the macroeconomic effects of the pandemic. First, through the general equilibrium effect, a higher degree of substitution will help mitigate the drop in aggregate consumption. Second, if we further allow the consumption behaviors to endogenously affect the infection, higher substitutability across sectors also reduces the infection risk exposure as a whole. Although our model does not incorporate both mechanisms, these effects are rather self-explanatory.

Figure A.10: Impulse Responses of the Economy to An Infection Shock: Different EOS between Contact and Non-contact Consumption



Note: This figure compares the impulse responses of the economy following a 10% increase in the top one third most influential nodes in the economy at time $t = 0$ under degree of elasticity of substitution between two sectors. The variables are average local infection ξ , average perceived transmission $\tilde{\psi}^{av}$, average total consumption c , and average contact-based consumption c_c .